Powder metallurgy approach to investigate the effect of Olive tree ash on Physio-Mechanical, Corrosion and Tribological properties of Aluminum matrix Composite

Erdachew Abiso Jatana

A Thesis submitted to the Department of Materials Science and Engineering

School of Mechanical, Chemical, and Materials engineering

Presented in Partial Fulfillment of the Requirement for the Degree of Master's in Materials Science and Engineering

Office of Graduate Studies

Adama Science and Technology University

June; 2023

Adama, Ethiopia

Powder metallurgy Approach to investigate the effect of Olive tree ash on Physio-Mechanical, Corrosion and Tribological properties of Aluminum matrix Composite

Erdachew Abiso Jatana

Advisor: Getinet Asrat Mengesha (Ph.D.)

Co-adviser: Devendra Kumar Sinha (Ph.D.)

A Thesis submitted to the Department of Materials Science and Engineering

School of Mechanical, Chemical, and Materials engineering

Office of Graduate Studies

Adama Science and Technology University

June; 2023

Adama, Ethiopia

DECLARATION

I hereby declare that this Master Thesis entitled "**Powder metallurgy approach to investigate the effect of Olive tree ash on Physio-Mechanical, Corrosion and Tribological properties of Aluminum matrix Composite**" is my original work. That is, it has not been submitted for the award of any academic degree, diploma, or certificate in any other university. All sources of materials that are used for this thesis have been duly acknowledged through citation.

Erdacew Abiso Jatana	____________________	_________________
Name of student	Signature	Date

Approval Page of M.sc. Thesis

We, the advisors of the thesis entitled "**Powder metallurgy approach to investigate the effect of Olive tree ash on Physio-Mechanical, Corrosion and Tribological properties of Aluminum matrix Composite**" and developed by Erdachew Abiso Jatana., hereby certify that the recommendation and suggestions made by the board of examiners are appropriately incorporated into the final version of the thesis.

Getinet Asrat Mengesha (Ph.D.)	________________	________________
Major Advisor	Signature	Date
Devendra Kumar Sinha (Ph.D.)	________________	________________
Co-advisor	Signture	Date

We, the undersigned, members of the Board of Examiners of the thesis by Erdachew Abiso Jatana have read and evaluated the thesis entitled "**Powder metallurgy approach to investigate the effect of Olive tree ash on Physio-Mechanical, Corrosion and Tribological properties of Aluminum matrix Composite**" and examined the candidate during the open defense. This is, therefore, to certify that the thesis is accepted for partial fulfillment of the requirement of the degree of Master of Science in Materials Science and Engineering.

Temesgen Debelo(Ph.D.)	_____________________	___________________
Chairperson	Signature	Date
Shimels Lema (Ph.D.)	_____________________	___________________
Internal Examiner	Signature	Date
Belete Sirabizu(Ph.D.)	_____________________	___________________
External Examiner	Signature	Date

Finally, approval and acceptance of the thesis are contingent upon the submission of its final copy to the Office of Postgraduate Studies (OPGS) through the Department Graduate Council (DGC) and School Graduate Committee (SGC).

Gebisa Bekele (Ph.D.)	_____________________	___________________
Department Head	Signature	Date
_____________________________	_____________________	___________________
School Dean	Signature	Date
_____________________________	_____________________	___________________
Office of Postgraduate Studies, Dean	Signature	Date

ACKNOWLEDGEMENT

First and foremost, I would like to express my heartfelt gratitude to the almighty God and his mother for providing me with the strength and health I needed to finish my studies. I would like to express my heartfelt appreciation to my advisor, Dr. Getinet Asrat Mengesha, and co-advisor, Dr. Devendra Kumar Sinha, for their unwavering support of my M.Sc. studies and research, as well as their patience, motivation, enthusiasm, and deep understanding.

My heartfelt gratitude also goes to the Materials Science and Engineering department's head, Dr. Gebisa Bekele, and the department's personnel as a whole.

I would like to express my gratitude to Ethiopian Defense University Institute of Research and Development for giving me scholarship and support by funding my thesis work. Also, I would like to extend my gratitude to the commandant of Ethiopian Defence University, Institute of Research and Development Colonel Yeshgat Adimassu (Ph.D.) for his good will, and Institute of Research and Development as a whole.

Last but not least, I would like to thank my classmates and lab assistants specially Demeke Tesfaye. Finally, thanks to Elias M., Yared G. and mechanical department as a whole for their support.

TABLE OF CONTENTS

CHAPTER PAGE

LIST OF TABLES

LIST OF FIGURES

TABLE PAGE

LIST OF ACRONYMS

Abbreviation	Description
AASTU	Addis Ababa Science and Technology university
ASTU	Adama Science and Technology University
Al	Aluminum
AMMC	Aluminum Metal Matrix Composites
ASTM	American Society for Testing and Materials
BHN	Brinell Hardness Number
CMC	Ceramic Matrix Composites
CTE	Coefficient of Thermal Expansion
DOF	Design of factor
DTA	Deferential Thermal Analysis
EDA	Energy Dispersive Analysis
EDS	Energy Dispersive X-ray Spectroscopy
EIS	Electrochemical impedance spectroscopy
FTIR	Fourier Transfer Infrared Ray
GRA	Gray Relational Analysis
Gr	Graphite
HV	Vickers Hardness
Mg	Magnesium
MMC	Metal Matrix Composites
MPa	Mega Pascal
OTA	Olive Tree stem Ash
PM	Powder Metallurgy
TGA	Thermo-Gravimetric Analysis
Wt.%	Weight percentage
XRD	X-Ray Diffraction

ABSTRACT

In recent years, there has been a significant increase in the use of aluminum matrix composites specially in, automotive, aerospace, marine and other structural applications. In this study aluminum matrix composites (AMCs) were fabricated by using different weight percentages of olive tree stem ash as a primary reinforcement and additives (Gr and Mg) by powder metallurgy processing technique. The fraction of olive tree stem ash (OTA) ranges from 3 to 9 wt.% at 3 wt.% intervals. whereas, additives were 1 wt.% Mg, and 3 wt.% Gr according to the recent literature review. In the first, the production of Aluminum matrix reinforced with 0 wt.%, 3wt.%, 6wt.% and 9wt.% of OTA and 3wt.% Gr with 1wt.%Mg with varying sintering temperature of 400^0C, 500^0C *and* 600^0C *for 2hrs. In the second, characterization and testing of OTA and AMC performed. Characterizations performed were thermal analysis TGA/DTA, XRD for phase analysis, FTIR for functional group (bonding condition) identification, SEM for wear surface morphological examination, and testing physio-mechanical (hardness and compressive strength), tribological and corrosion test for fabricated samples were done. Next, Optimization using Taguchi Multi-Response Grey Relational Analysis* L_{27} *orthogonal array to determine the influence of powder metallurgy (PM) process parameters (compacting Pressure, sintering temperature and sintering time) with varying composition of OTA. Finally, results of characterization and tests were discussed. The XRD results of composites indicates that all fabricated AMCs contain Al as a major peak and minor peaks of reinforcements and additives at 9wt.% of OTA. It also confirmed absence of intermetallic peak. Increasing the wt.% of OTA decreased density of the composite and maximum hardness and compressive strength obtained at 9wt.% of OTA sintered at* 600^0C *for 2hrs. Hardness and compressive strength enhanced that of pure matrix material 54.2l% and compression by 52.5% The resistance of wear loss and corrosion increased when wt.% OTA increase up to certain limit, then decreased. The confirmation test result of optimized sample revealed that the optimized one had greatest physio-mechanical properties than other* L_{27} *samples. Hence this AMC will be suitable for potential application in automotive, aerospace, defense, marine and structural application.*

Key words: *Aluminum matrix, corrosion, Olive tree ash, physio-mechanical, Powder metallurgy, tribological*

CHAPTER ONE

1. INTRODUCTION

1.1. Background of study

Composite materials have recently drawn a growing amount of interest due to their unique characteristics and potential for use in a range of applications(Kanda et al., 2018). The requirement for lightweight materials with high strength and stiffness is one of the key factors driving the development of composite materials. Weight reduction is crucial in many applications to increase efficiency, save costs, and improve performance. Because composites have a high strength-to-weight ratio, composite materials are a great option for lightweight structures(Srivastava, 2017).

Currently researchers have turned to search for new materials that will meet all the requirements of industries spanning air transportation, ground transportation, marine transportation, defense-related products and even a plethora of commercial products including sporting goods(Gürleme, n.d.; Kareem et al., 2021; Shahid & Scudino, 2018; Shanmugavel et al., 2022; Vijayaram & Baskaralal, 2016). MMC exhibit attractive properties such as good hardness, better yield strength, strength-to-weight ratio, low coefficient of thermal expansion, superior wear, and corrosion resistance (H. I. Akbar et al., 2020a; Hayajneh et al., 2019; Kumar Sharma et al., 2020; Parveez et al., 2021; Vani & Chak, 2018; Zeren, 2015). Due to their excellent combination of properties, MMC's are a significant class of advanced engineering materials that are rapidly replacing conventional metallic alloys in a variety of industries, including the aerospace, and automotive sectors as well as the sports and recreation, marine, and defense sectors(Khatkar et al., 2018; Srinivasan et al., 2020).

Aluminum metal matrix composites are well suited for the aerospace, automotive, marine and military sectors due to their low density, high specific strength and stiffness, improved wear resistance, and controlled expansion coefficient(Geng & Huang, 2014). By suitable use of different reinforcements, the Aluminum metal matrix can be used to achieve a wide range of property combinations such as improved physio-mechanical, wear, tribological and corrosion resistance properties, reducing production costs and adapting to new generation technologies. It is thought that the limited mechanical properties of aluminum and its alloys have an adverse effect on its utilization in applications for the automotive, aerospace, and other industries. Thus, several types of reinforcements are added to aluminum and its alloys to improve their physio-mechanical properties based on the desired mechanical properties(Yekinni et al., 2020).

Quest for low cost, pollution regulations and growing fuel costs have forced the automotive industry to develop lighter and more fuel-efficient vehicles(Karaoglu et al., 2021). Vehicle weight reduction can increase overall environmental protection, decrease greenhouse gas emissions, and increase fuel efficiency(W. Zhang & Xu, 2022). Every 10% reduction in weight from the typical car or light truck can result in a 6-9% reduction in fuel consumption, and a reduction of 100 kg in net load can result in a reduction of fuel consumption by half a liter every 100 km and 2000 kg fewer CO_2 are produced during the average life of an automobile as a result(Cheah, 2010; Ibhadode, 2022).

No studies have been conducted on the characteristics of composites made of graphite, OTA and aluminum via powder metallurgy. By producing a graphite-rich lubricating coating between the sliding surfaces, graphite was added to these composites to increase their tribological capabilities and seizure resistance features. Al-graphite composites are employed in the automotive sector as piston, cylinder lining, and electronic packaging materials(Liu et al., 2010; Omrani et al., 2016). Because graphite has a lubricating effect. Al-graphite composites with an aluminum matrix supplemented with ceramic particles perform better due to lower friction coefficient values, low coefficient of thermal expansion and reduced wear(Baradeswaran & Perumal, 2014; Faleh, Muna, Ştefănescu, et al., 2015).

The options for AMC development have led to numerous research efforts directed at employing both agro and industrial products as reinforcements to improve mechanical, physical and tribological properties(You et al., 2022). The recent projections of ecofriendly, locally available, sustainable, future green and renewable manufactured goods indicate increase in use of agricultural and industrial products(Rahman et al., 2023). Majority of developing countries in world are rich in agricultural resources. Some of costly synthetic reinforcement like SiO_2, SiC, TiC, and other ceramic oxides as well as carbides which are not produced in developing countries. These necessitate the need to source locally available materials to reduce the cost of production of aluminum composite affirmed that in recent times, by the use of ashes gotten from the conditioning solid agro-products like coconut shell, palm kernel shell, bamboo leaf, and groundnut shell (Kulkarni et al., 2019; You et al., 2022) used for reinforcement in the production of low cost aluminum based composites(H. Akbar et al., 2020).

The property requirements, cost factors, and possible future applications are taken into account when choosing the processing method(Vijayaram & Baskaralal, 2016). AMC-based can be fabricated using various methods depending on the desired properties and end-use applications. Powder Metallurgy, Stir Casting, Squeeze Casting, Rheo-casting, Plasma Vapor Deposition and Infiltration Technique are processing methods.

One of the most commonly used fabrication methods for aluminum-based MMCs is stir casting, which involves the incorporation of reinforcement particles into a molten aluminum matrix through stirring. The mixture is then solidified to produce a composite material. Stir casting is a relatively simple and cost-effective method that can produce composites with a wide range of reinforcing materials and compositions. It is commonly used for the production of low to medium strength and stiffness composites with good ductility and toughness.

But there are challenges in fabricating MMCs using stir casting such as poor wettability between the reinforcement and matrix(S. Sharma et al., 2022), undesired reactions between the matrix and the reinforcement(Torralba et al., 2003), inhomogeneous distribution of reinforcement particles(Chen et al., 2016), particle clustering and sedimentation(Vijayakumar et al., 2022), and formation of undesirable phases(Wang et al., 2019). Another widely used method for the production of aluminum-based MMCs is powder metallurgy. This method involves mixing aluminum powders with reinforcement particles, followed by compaction and sintering to produce a composite material. Powder metallurgy enables the fabrication of composites with complex shapes and sizes, high strength and stiffness, and good wear resistance and thermal conductivity. PM processing can overcome stir casting challenges like formation of undesirable phase formation due uncontrolled temperature during cooling.

The parameters that determine the MMC manufacturing procedures employed include the type and composition of the matrix and reinforcement material, the wettability and uniform distribution of the reinforcing particle in the base matrix(Samal et al., 2020), and the production cost(Aynalem, 2020).

Porosity, non-homogeneous distribution of particle reinforcements(Mohanavel et al., 2018; P. Sharma et al., 2016), wettability, and a chemical reaction between the reinforcement and matrix are only a few issues that stir casting encounters. Like Gr with low density, which floats in the melt, lead to weak bonds between Gr particles and the matrix (Mohanavel et al., 2018).

1.2. Statement of the problem

Environmental concern, better performance, fuel efficiency, emergence of electric vehicles, rise in fuel price and government regulations on emissions are the most important issues enforcing the automotive, aerospace, marine, and defence industries to enhance performance (Czerwinski, 2021; Miller et al., 2000). To enhance performance, modification of automotive parts is important issue to improve its efficiency. One of the best ways to improve efficiency is weight reduction and using non-costly materials. Lack of supply and increasing cost enforced researchers to focus on recycling technique. Environmental benefits, cost savings, improved properties and sustainability are the major advantage of using agro-waste(organic materials) and industrial waste as reinforcement (H. Akbar et al., 2020; Velusamy et al., 2022). Shortage of supply and increment in cost made researchers to give more attention on reusing agro-waste (organic materials) and industrial solid waste as reinforcement. Hence, using alternative reinforcing materials that are inexpensive, easily accessible, and physical and mechanical properties equal to conventional particulates is crucial point(H. Akbar et al., 2020). Aluminum alone or its alloy does not provide the required properties under all service conditions(Kumar Sharma et al., 2020; Nturanabo, Leonard Masu and John Baptist Kirabira, et al., 2020). To overcome these functionality-related properties reinforcing is used. In addition to their low cost, organic materials and industrial solid waste reinforcements play great role in weight reduction, increased composite life, and improved recyclability. Hence it becomes imperative to promote the viability of these groups of materials by utilizing cost-effective metal matrix and reinforcements. No research works done on olive tree stem ash reinforced aluminum matrix composites to investigate the physical, mechanical, wear, and corrosion property via powder metallurgy. PM ensures a uniform microstructure, good wettability between the matrix and reinforcement, and inhibits the production of any unwanted phases in the manufactured MMC(Dev Srivyas & Charoo, 2018; Vani & Chak, 2018).

Liquid metal processing has disadvantages like low wettability, limited control over microstructure, use high temperature and limited range of reinforcement materials. This work aimed to study the effect of olive tree ash on physio-mechanical, corrosion and tribological properties of aluminum matrix composites via-powder metallurgy.

1.3 General Objective

The general objective of this study is to investigate the effect of Olive tree ash on Physio-Mechanical, Corrosion and Tribological properties of Aluminum matrix Composite via Powder metallurgy approach.

1.3.1. Specific objectives

- To prepare olive tree ash from olive tree stem
- Preparing samples from OTA reinforcement with Mg and Gr(as additives) in aluminum matrix composites via powder metallurgy route.
- Characterizing the physio-mechanical, tribological, corrosion, and tribological behaviors of the manufactured composites
- Comparing the physio-mechanical, wear, and corrosion, behaviors of the pure(unreinforced) Al and fabricated aluminum matrix composites.
- Optimization of the PM process parameters (OTA composition, compacting pressure, sintering temperature and sintering time) by using Taguchi based grey relational multi response optimization method.

1.4. Significance of study

i. More understanding of powder metallurgy techniques in developing aluminum matrix composites.
ii. A reduction in the overall weight of the material, and used as (filler)substitute for high cost ceramic reinforcements.
iii. Understanding the PM processing.

1.5. The Scope of Study

This research wok covers introduction, a literature review that covers the essential problems, and recent published work in the field of aluminum matrix composites with additive (graphite) and solid agro-waste products and processing methods. In introduction, MMC material in general and AMCs in specific.

Next, review on related latest works on aluminum matrix composite reinforced with graphite and agro-waste solid reinforcements. Then preparation of composite powders, fabrication methods, testing and characterization were included. Selecting optimal compositional mixtures, high energy planetary ball milling, the consolidation of powder composites into solid compacts, the parameters of sintering temperature and time, and then density measurement, Vickers microhardness, microstructural analysis, compression testing, corrosion rate measurements, and pin on drum wear testing. Also, Taguchi GRA based multi-response optimization included. Finally, a conclusion and recommendations for future work on the most important improvements and findings of fabricated composite discussed.

1.6 Thesis organization

This study consists five chapters and highlight of each chapter is blow. **In the first chapter** introduction and background of study, problem statement, objectives, significance of research and scope, limitation of the work, output of work and the organization of the thesis. T**he second chapter** is organized for the literature review on thesis related studies. About composite material and its processing methods. Effect of reinforcements on physio-mechanical, tribological, wear and corrosion properties. Finally, research gap included. **The third chapter** includes materials used and methodology. Under this chapter reinforcement preparation, process of fabrication, characterization and tests are covered. In the **fourth chapter** detail discussion and analysis of results based on the result from third chapter. Finally, **fifth chapter** present the conclusion and recommendation of future works.

CHAPTER TWO

2. LITERATURE REVIEW

2.1. Composite materials

A composite is mixture of two or more constituents or phases that are chemically distinct on a microscopic scale, separated by a distinct interface, and can easily be specified(Nturanabo et al., 2019; A. K. Sharma et al., 2020a; G. Singh et al., 2017). The constituents retain their identities in the composite; that is, they do not dissolve or otherwise merge completely into each other, although they act in concert(Seetharaman & Gupta, 2021a). Composites are one of the most widely used materials because of their adaptability to different situations and the relative ease of combination with other materials to serve specific purposes and exhibit desirable properties. In addition, other criteria are normally satisfied before a material can be called a composite. The constituents have to be present in reasonable proportions, and the constituent phases should have distinctly different properties, such that the properties of the composite are noticeably different from the properties of the constituents (Nturanabo, Masu, et al., 2020).

Composite materials are usually classified according to the physical or chemical nature of the matrix, e.g. metal matrix, polymer matrix, and ceramic composites(A. K. Sharma et al., 2020b). Additionally, the emergence of the intermetallic matrix and carbon matrix composites was reported by (Raju, 2019).

2.2. Classification of composite materials

Depending on variables including the type of reinforcement, matrix material, and application, composite materials can be categorized in a variety of ways. Composite materials can be classified based on the matrix phases and types of reinforcement phases in the matrix phase(D. Kumar et al., 2019). Metal matrix composites (MMC), ceramic matrix composites (CMC) and polymer matrix composites (PMC) are the various types of composites based on matrix phase.

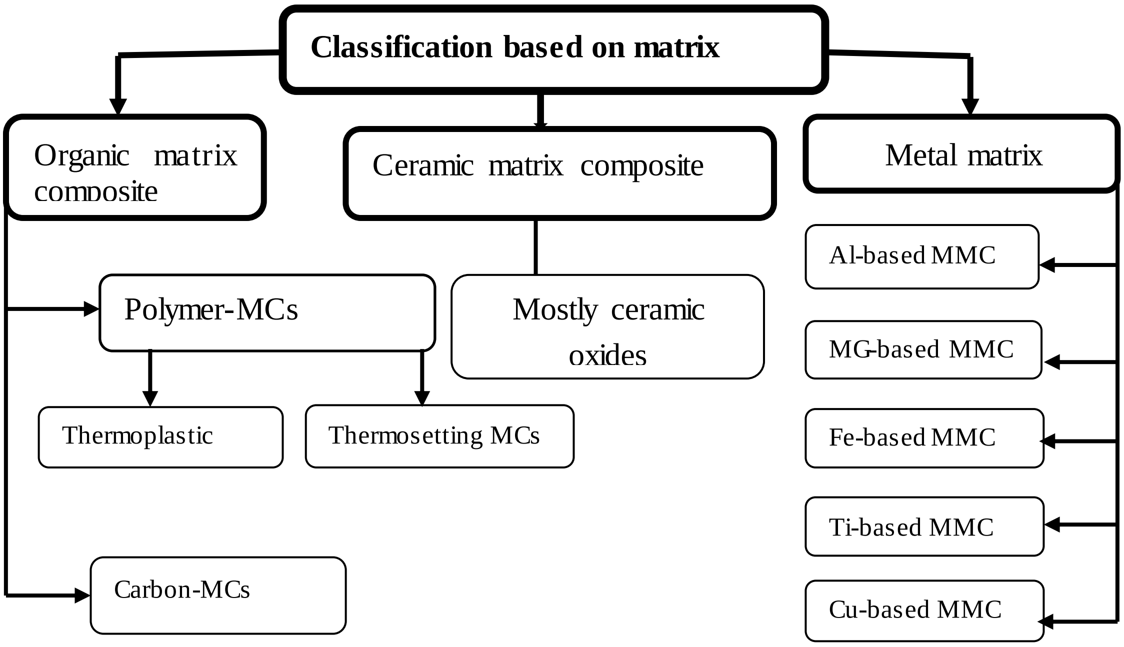

Figure 1. Classification of composite materials based on matrix(Ashebir et al., 2022a; Buckner et al., 2016; Seetharaman & Gupta, 2021b)

Organic matrix composites (OMCs), MMCs, and Ceramic matrix composites are the three main categories of composite materials based on matrix(Ramanathan et al., 2019). In general, it is assumed that the term "organic matrix composite" refers to two subclasses of composites: polymer matrix composites (PMCs) and carbon matrix composites, also known as carbon-carbon composites.

MMCs are made by dispersing a reinforcing material into a metal matrix(J. Singh & Chauhan, 2015). MMCs usually consist of lightweight and low-density metal, such as aluminum or magnesium, reinforced with particulate or fibers of a ceramic material, such as SiC or Gr(Mussatto et al., 2021). Compared to unreinforced metals, MMCs offer higher specific strength and stiffness, higher operating temperature, and greater wear and corrosion resistance, as well as the opportunity to tailor these properties for a particular application.

2.2.1. Metal matrix composite

MMCs are interfused materials that reveal qualities that are difficult to acquire from a single material, such as high strength and stiffness with low density(Lindroos & Talvitie, 1995). Engineering materials known as MMCs have a metal matrix that has a sturdy ceramic reinforcement added to it to enhance the characteristics.

MMCs combine the ductility and toughness of matrix alloys with the strength and stiffness of ceramic reinforcements, resulting in increased strength in compression and shear as well as increased service temperature capabilities.

MMCs are metals or metal alloys that incorporate particles, whiskers, fibers or hollow micro balloons made of a different material and offer unique opportunities to tailor materials to specific design needs. In automotive applications, for example, these materials can be tailored to be light-weight and with various other useful properties including high specific strength and specific stiffness, high hardness and wear resistance, high thermal conductivity, high energy absorption and a damping capacity and low coefficients of friction and thermal expansion. The matrix is the monolithic or base material, which may be an alloy of Al or a pure metal such as Al (Rajak et al., 2019). A lighter metal, such as Al, Mg, Cu, or Ti, serves as the matrix in structural applications and acts as a guide for reinforcement.

2.2.2. Classification of MMCs based on types of reinforcements

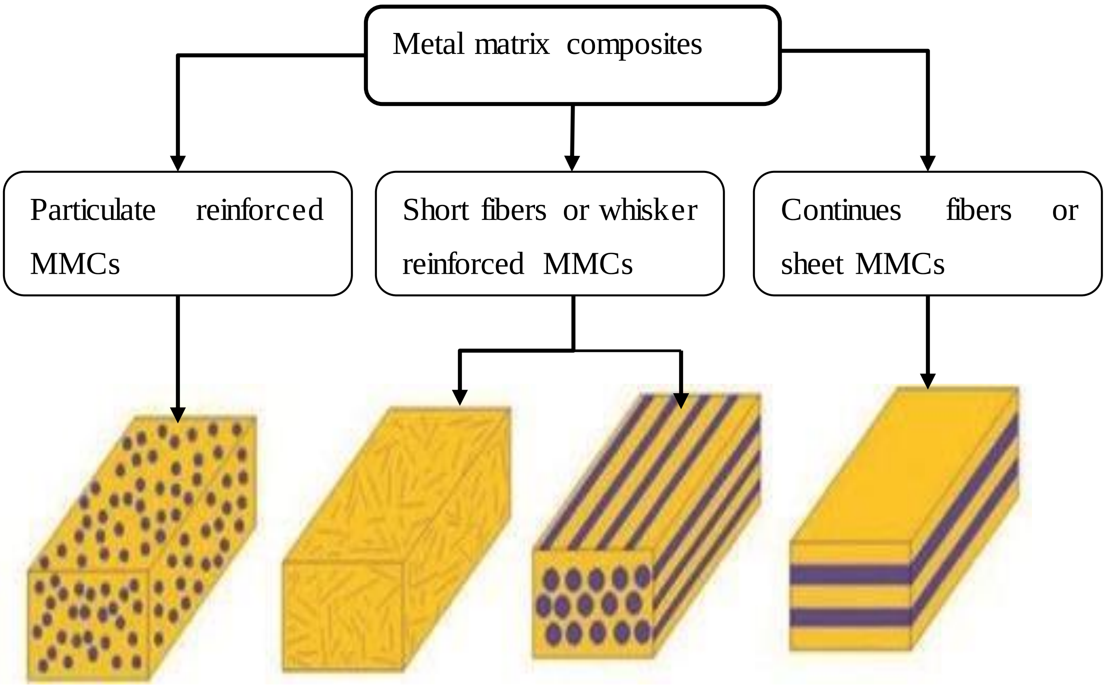

Figure 2. Classification of composite materials based on reinforcement type

Particulate reinforcements on AMCs

Particulate-reinforced MMCs are currently the most extensively researched and used MMC type, primarily because of the property improvements that can be achieved, the low cost and availability of particulate materials, and the processing adaptability of particulate-reinforced MMCs to conventional technology(Ashebir & Science, 2021).

2.3 Manufacturing and processing methods of metal matrix composites

Different types of manufacturing methods are used to make MMCs. The MMCs' ultimate qualities are heavily influenced by the manufacturing process. The MMC-specific qualities, volume of production, cost, matrix, distribution of reinforcement components (particles or fibers), and product application areas all play a role in the method selection process. Depending on how hot the metallic matrix gets during processing, different processing techniques used to make particle reinforced MMCs can be categorized.

Processing of MMC can be classified into three main categories: Solid state processes

- Solid State Processing
- Liquid State Processing
- In-Situ Processing

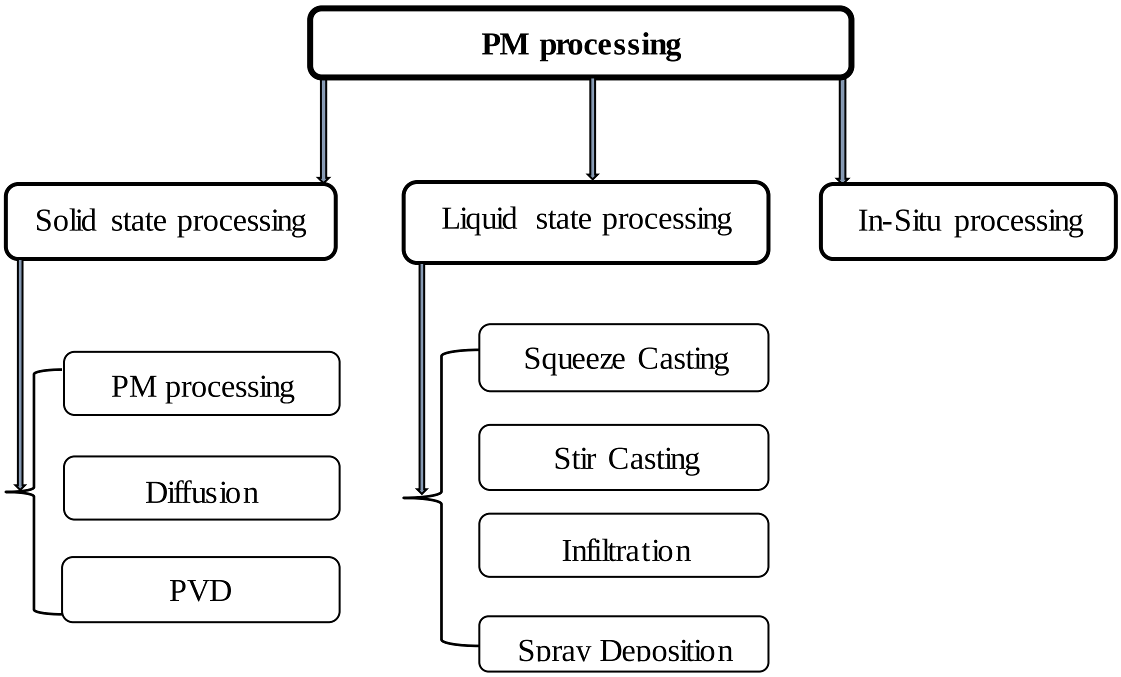

Figure 3. Powder metallurgy processing methods(Surappa M.K., 2003)

2.3.1 Solid State Processing

MMCs are made by a method known as solid state fabrication in which the matrix metal and dispersion phase are joined together as a result of mutual diffusion that takes place between them in solid states at high pressures and temperatures.

Due to its ability to do away with the necessity for secondary procedures, powder metallurgy is sort of likely the most effective method for making complex components and parts with a close net form. For pieces with complicated architecture, PM offers a variety of uses and nice dimensional tolerance(Ravindran et al., 2022). There are other strategies for creating particulate reinforced MMCs, however the PM pathway is one of the most cost-effective ways to create near net particle reinforced MMCs. One of the best ways to obtain the desired qualities, such as less porosity and more uniform reinforcement distribution, is through the use of powder metallurgy(Sankhla et al., 2022). Additionally, it provides adaptability and flexibility in the choice of process parameters, including compaction pressure, holding time, sintering thereby increasing the mechanical properties. Metal powder is mixed with ceramic whiskers, short fibers, or particles either dry or wet. The combination is then put through additional processing after blending, including cold compaction, canning, degassing, and high temperature consolidation. Discontinues ceramic whiskers and metal powder are combined.

2.3.2 Powder Metallurgy Processing

In order to lessen the wettability or interfacial reactivity issues that are frequently associated with liquid processing, the PM approach for the manufacturing of AMCs had been developed(Vani & Chak, 2018). As a further benefit, this method also enhanced the spatial distribution of particulates in discontinuously reinforced AMCs.

Powder blending: One of the primary phases in PM is powder blending, which involves using a ball mill to combine powder from several materials with various mechanical and chemical qualities into a single form. Particle size reduction (breaking down the material), mixing or blending, and particle shape are the three main goals of the milling procedure. The process of blending results in shape homogeneity and the homogeneous mixing of powder particles, which gives the material a variety of mechanical qualities with consistent features(John & Menezes, 2021). By compressing the particles using a compression force kind of operation, the particles are broken into fine particles. A solid lubricant is blended or combined with the fine granules to provide sufficient fluidity.

Ball milling is a method of grinding that uses balls made of hard materials like steel or ceramics to grind the powder combination. The powder mixture is normally put in a ball mill.

The balls are driven by the mill's spin, and as they strike the powder mixture, they do so with high-energy impacts that reduce the size of the particles and alter the crystal structure.

Powder compaction: A press or compacting machine is used to compress metal particles into the proper shape and density as part of the crucial powder compaction process in powder metallurgy(N. Kumar & Bharti, 2021). The metal powders are put in a die during the compaction process and put under a lot of pressure, which makes the individual particles bend and stick together.

Sintering: Performed at controlled atmosphere to bond atoms metallurgically; Bonding occurs by diffusion of atoms; done at 70% of abs. melting point of materials It serves to consolidate the mechanically bonded powders into a coherent body having desired on service behavior. Densification occurs during the process and improvement in physical and mechanical properties are seen.

2.4 Effects solid lubricant on wear properties of MMCs

The primary reason for the superior lubrication properties of solid lubricants is their ability to shear through the mating surface, and their lubricious behavior can be correlated to their layered structure(John & Menezes, 2021). (Lakshmi Narayana et al., 2021) investigated how graphite affect the mechanical characteristics of aluminum matrix composites. They discovered that adding graphite increased the composites wear resistance. The strengthening impact of the graphite and the enhanced interfacial connection between the matrix and the reinforcement were credited with the improvements.

Graphite was included to improved seizure resistance features and tribological properties by forming a graphite-rich lubricant film between the sliding surfaces. For these reasons composites Al-graphite are used in automotive industry as piston and cylinder liner materials(Faleh, Muna, & Ştefănescu, 2015).

Gr is a low-density(Dipl-ing et al., 2012), solid-lubricant 3D carbon material. Within AMCs, Gr attends as a solid lubricant between the composite and rubbing surface to assist in the reduction of composite wear without the need for conventional solid and liquid lubrication(Jinfeng et al., 2009). The proper material selection is critical to (1) ensuring that the solid lubricant areas are not sheltered by wear debris and (2) allowing the development of lubricating transfer films at the tribo-interface.

Finally, the advantage of self-lubricating composites over thin solid lubricating films deposition on ceramic substrates is the ability to have an infinite source of solid lubricant, which has been sustained as the matrix material wears. When compared to the material deposited by solid lubricant films, which fail after the film has worn away, self-lubricating matrix composites reduce the possibility of failure. Self-lubricating composite materials can withstand low friction and wear without the need for external lubricants(Rohatgi, n.d.). The incorporation of Gr particles reduces the coefficient of friction and wear rate of Gr particle reinforced metal and ceramic matrix composites compared to similarly unreinforced material(Rohatgi, n.d.). With increasing Gr particle wt.%, the matrix composite's friction and wear rate decrease. The Gr particles were discovered to be superior to other lubricant particles, and they provided efficient lubrication when used at high temperatures.

Typical Applications of Solid Lubricants

- ✓ When conventional lubricants are inadequate the solid lubricants are useful especially for reciprocating motion, for example, in gear and chain lubrication mechanisms. Also, prevent from various corrosion mechanisms.
- ✓ Substitutes for chemically active lubricants additives.
- ✓ Extreme temperature and oxidizing environmental conditions.
- ✓ High loading capabilities

2.5 Solid-Waste Particulate Reinforced AMCs and HAMC

Use of solid waste ashes as reinforcing particles in metal matrices to enhance strength qualities, in AMCs is growing in popularity. AMCs can be strengthened with agro-industrial solid wastes. The use of waste materials as reinforcement can contribute to sustainability efforts by reducing waste disposal(Dwivedi et al., 2020) and promoting the use of renewable resources and simultaneously lowering the cost of product production. These are many solid waste materials that can be utilized as reinforcement for MMCs, and they are often divided into three categories: industrial solid wastes, agricultural solid wastes, and post-consumer solid wastes.

Recently, several investigations on AMCs that utilize bagasse ash, bamboo leaf ash, coconut shell ash, palm oil fuel ash, and rice husk ash have been carried out. Some of these solid wastes are used as animal feed, while others are dumped and burned at public landfills, both of which are harmful to the environment. Currently most of the research going on Agro-

Waste, as they are easily available, low cost, low density, reduce environmental pollution(Virkunwar et al., 2018). These agro-waste ashes often contain a high percentage of silica (SiO_2) with a distribution of other refractory oxides such as Al_2O_3 and hematite. Numerous researchers studied that Agro-waste derivatives like bamboo leaf ash (BLA), rice husk ash (RHA), bagasse ash (BA), palm kernel shell ash (PKSA), maize stalk ash (MSA), corn cob ash (CCA), bean shell waste ash (BSWA) can be used as reinforcing material improving the Mechanical & Tribological Properties of AMCs(Parveez et al., 2021; Virkunwar et al., 2018).

2.6 Tribological and Corrosion Behaviour of AMCs

The gradual removal of material from solids surface is termed as wear. Wear is a continuous loss of material due to rubbing action between the two contacting surfaces. Wear may be due to micro-cracks or by localized plastic deformation. Wear may be due to many physical, mechanical or chemical phenomenon. Abrasive, adhesion, corrosion, oxidation, fretting, fatigue and erosion are the different kind of wear that leads to material removal. It is difficult to completely nullify the effect of wear, but we can reduce the friction and wear by means of lubrication, by formation of smooth surface, by modification of components material rubbing against each other and by correct assembly of fitted components parts. Aluminum have two basic wear mechanisms i.e. oxidation mild wear and metallic severe wear(Srivyas & Charoo, 2018). Many studies are conducted in order to investigate the effect of applied load, sliding velocity and composition on seizure resistance. The wear behavior of the composite was higher when compared to the base matrix. The unreinforced aluminum was softer than composite. This enhancement in the wear resistance was because of: the large hardness, which restricts plastic flow during the sliding condition, and powerful interfacial bonding between reinforcement particle and matrix phase. The wear resistance of the composites increased with the addition of the of silica reach organic ash (Kulkarni et al., 2019). The best wear resistance was obtained with the use of rise husk ash(containing 73.5% alumina, 25% RHA and 1.5% graphite)(Alaneme & Sanusi, 2015).

Corrosion performance of bamboo leaf ash reinforced hybrid composites in 3.5% NaCl showed better corrosion resistance(Seetharaman et al., 2022).

Table 1. Summary of AMC properties

No	Matrix	Reinforcement	Fabrication method	Tests used for study of Physio-mechanical property	Significance	Reference
1	Al	Gr.	Stir casting	compression strength, and micro hardness	Increased compressive strength	(Taiwo et al., 2020)
2	Al	Gr. And Egg shell	PM	Hardness and compressive	Best compressive strength and hardness	(Almomani et al., 2020)
3	Al	Gr. And Mg	Stir casting	Hardness and wear rate	Hardness increased, decreasing wear	(Khatkar et al., 2018; Panda et al., 2019; P. Sharma et al., 2017)
4	Al	Gr.	PM	Hardness and wear rate	Hardness increased, decreasing wear	
5	Al	Gr. And coconut shell ash	Stir casting	Hardness and density	improved hardness and ultimate tensile strength of the composites	

2.7 Research gap

From the review, reinforcement materials such as ceramic particles, SiO_2, SiC, Al_2O_3, Gr, and agro-industrial solid wastes such as fly ash, rice husk ash, and sugar cane bagasse ash were used to enhance physio-mechanical, and tribological, corrosion properties of AMCs. Many solid agro-waste ashes were jointly used with solid lubricants like (Gr and MoS_2) and hard ceramics to alter physio-mechanical, wear, tribological and corrosion behavior of aluminum matrix. But no research work has been conducted to study the effect of olive tree ash on pure aluminum matrix, reinforced with additives like graphite and magnesium by powder metallurgy processing method. This study focused on the effect of locally available olive tree ash on aluminum matrix by varying olive tree ash composition with graphite and magnesium particulates by using powder metallurgy processing method.

CHAPTER THREE

3. MATERIALS AND METHODS

3.1 Materials

Materials used in this study were Gr and Mg as additives, olive tree ash reinforcement and aluminum as matrix.

Figure 4. Raw materials used for this research work

Table 2. Raw materials and reasons for selection.

No	Raw materials		Reasons for selecting composite production	Reference
1	Matrix	Al	(i) Lightweight, and low density, but the low melting point hinders its use in the high-temperature application. (ii) High ductility, malleability, and toughness with low strength, soft, and low wear and friction resistance (iii) Low hardness and mechanical stability at high temperatures because of its low melting point which can be improved by improved reinforcing.	(Ashebir et al., 2022b)
		Gr	(i) Lightweight, low density (ii) Superior solid-lubricating material	(Srinivasan et al., 2020;

2	Additives		(iii) Low cost (iv) Low coefficient of friction, (v) Outstanding thermal conductivity (vi) Resistance to corrosion,	Taiwo et al., 2020)
		Mg	(i) Lowest density of all structural metals (ii) Its stiffness to weight ratio is very high (iii) The dimensional stability and damping capacity are high, it is easily(soft) machined and can be readily recycled	(Yamagata, 2003)
3	Reinforcement	OTA	(i) Low density, low cost harmless(non-toxic), eco-friendly, availability, biodegradability and can substitute for synthetic ceramic reinforcements like SiO_2.	(Alshammari et al., 2019a)

3.1.1 Physical and Mechanical Properties of prepared powders

Table 3. Physical and mechanical properties of materials used in this study (A. Zhang & Li, 2023)

Materials	Al	Mg	Graphite	OTA
Appearance	White	grey	Black	Black
Density (g/cm^3)	2.7	1.74	2.26	0.87 - 0.99
M.W. (or At. W)	26.98	24.31	12.01	-
Melting point. (°C)	660	650	3600	-
Thermal conductivity(W/m-K)	237	156	114	-
Particle grain size(μm)	≤ 50	≤ 50	≤50	≤50

Vickers hardness (Mpa)	33	32.5	67	Not applicable
Compressive Strength (Mpa)	2800	65–100	20-200	Not applicable
Tensile Strength (Mpa)	130-195	180-440	3 – 33	Not applicable
Young's Modulus (Gpa)	70	45	380 – 470	Not applicable
Purity (%)	99.5	99.5	98	Not applicable

3.1.2 Olive Tree Ash Preparation and characterization

Because of their availability and low cost, natural reinforcements, such as plant and mineral products, have been replacing ceramic, glass and carbon in recent years. Industrial and agricultural wastes that rich in oxide material can be used as an alternative material in metal matrix composite(H. I. Akbar et al., 2020b). Olive tree has attractive properties like it cannot be destroyed by termites and not easily decay in the soil. There are more than thirty types of olive tree(Ozturk et al., 2021). But its usage is limited because of hardness to use for construction (difficult for the nail to penetrate). These its attractive properties and limited usage initiated to conduct compositional analyses on olive tree stem to use as a reinforcement. The chemical composition of olive tree stems varies depending on several conditions such as origin, proportion of branches on the tree, storage conditions, climatic conditions, moisture content, and degree of contamination with soil. For this work olive tree stem from ASTU compound were used. Once the cutting operation done, leaves, barks and thin branches will be manually removed from the rest of the constituents. The steam the washed and air-dried in an oven for a week at 80^0C temperature and finally ground(milled) using a wood file. Next thermal analysis (thermogravimetric analysis) performed. Based on thermal analysis result the powder calcined at 850°C for two hours to remove moisture and organic matters like cellulose, lignin and others. In this operation, the olive tree calcined to obtain desired composition. After calcination ash's color changed from black to grey or slightly greyish-white. The calcined (heat treated) OTA grind by mortar and sieved based on requirement of ash size.

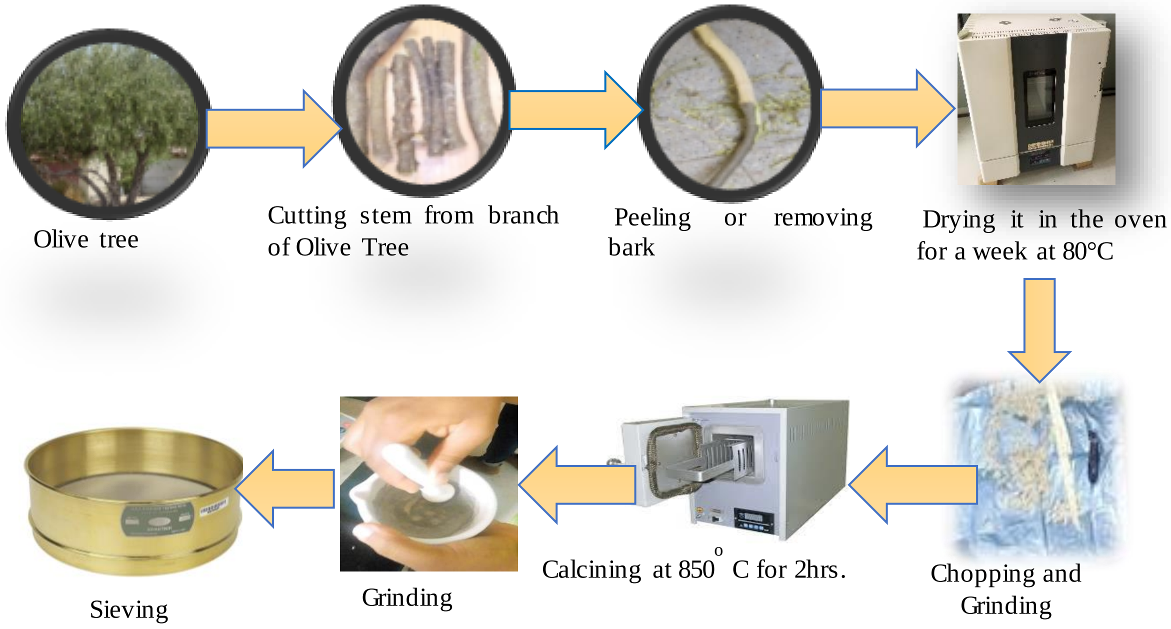

Figure 5. OTA preparation

3.2 Methods or Experimental procedure

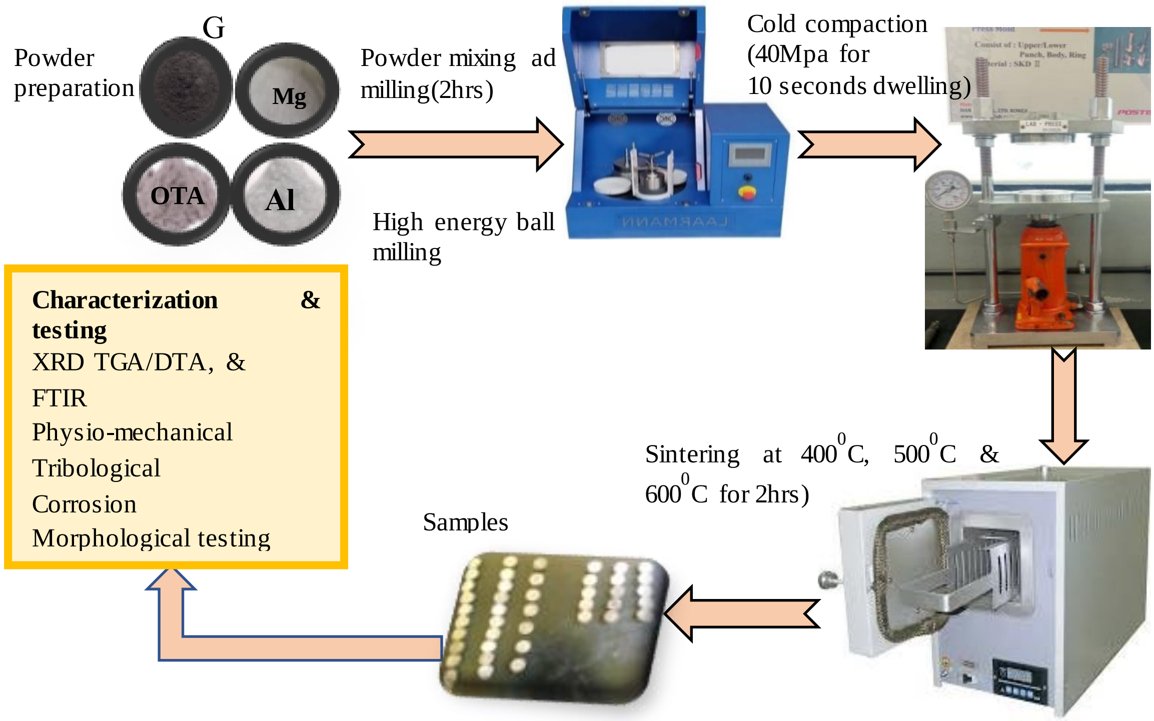

Figure 6. Methodology

3.3 Weight percent calculation and Sample design

In this research work Mg(1wt%) and Gr(3wt%) are used. Composition of each sample calculated based on the sum rule of composite. The pre-designed die and punch has the following dimensions. The inner diameter and length/height of the die is 16mm and 7mm respectively, whereas the punch diameter is 16mm with small clearance to insert it into the die during compaction of the powder by hydraulic pressing machine. Based up on the above dimensions, cylindrical specimen for Al matrix and reinforcements will be fabricated with a size of length (L) and diameter (d) as shown in the produced specimens' dimensions are limited to produce cylindrical specimen with short-length due to the capacity of the hydraulic pressing machine.

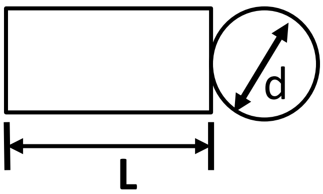

Figure 7. Dimension for specimen

The pre-designed die and punch will be used to manufacture the required number of specimens based on the following types of tests to be conducted;

- The Hardness, compression test and microstructural test specimen length is 7mm with 16mm diameter.
- The wear test specimen length is 12mm and 6mm diameter.

3.4 Experimental Design

Table 4. Experimental Design

Designation	MT. (hrs.)	CP. (MPa)	ST. (^oC)	St. (hrs.)	Al (wt.%)	Mg (wt.%)	Gr (wt.%)	OTA (wt.%)
Al	2	40	400, 500 & 600	2	100	0	0	0
A0OTA	2	40	400, 500 & 600	2	93	1	3	0
A3OTA	2	40	400, 500 & 600	2	90	1	3	3

A6OTA	2	40	400, 500 & 600	2	87	1	3	6
A9OTA	2	40	400, 500 & 600	2	96	1	3	9

MT- milling time, CP-compaction pressure, ST-sintering temperature and St- sintering time

3.6 Test and Characterization techniques used in this study

3.6.1 Density and porosity measurements

Density of composite measured to study the influence of the hybrid reinforcement's wt.% proportions on the densities of specimens produced. Experimental density measured to estimate the porosity levels in the composites. It is obtained by comparing the relative and theoretical densities of each weight ratios of composite produced. In this work Archimedes principle used to calculate actual (experimental density) at room temperature and theoretical density also calculated by using "Rule of Mixture" formula. Similarly, relative densities of the sintered samples will be measured using Archimedes method using water as a floating liquid according to MPIF standard in which the sintered specimen is weighed in air and in distilled water then the density($\boldsymbol{\rho}$) could be calculated according to the following equation in (g/cm^3):

$$\rho = \frac{w_{air}}{w_{air} - w_{H_2O}} \quad \text{.....} (1)$$

The experimental density for each composite will be evaluated by weighing the composite sample using a high precision electronic weighing balance with a tolerance of 0.001 mg. The measured weight in each instance is divided by the volume of the respective specimens. The theoretical density will be evaluated via the rule of mixtures given by:

$$\boldsymbol{\rho}_{Al/(Gr\text{-}Mg\text{-}OTA)} = \boldsymbol{wt\%}_{Al} \times \boldsymbol{\rho}_{Al} + \boldsymbol{wt\%}_{Gr} \times \boldsymbol{\rho}_{Gr} + \boldsymbol{wt\%}_{Mg} \times \boldsymbol{\rho}_{Mg} + \boldsymbol{wt\%}_{OTA} \times \boldsymbol{\rho}_{OTA} \quad \text{.....} (2)$$

Where; $\rho_{Al/(Gr\text{-}Mg\text{-}OTA)}$ is the density of the hybrid composites,

$wt\%_{Al}$ and ρ_{Al} are weight fraction and density of Al,

$wt\%_{Gr}$ and ρ_{Gr} are weight fraction and density of Gr,

$wt\%_{Mg}$ and ρ_{Mg} are weight fraction and density of alumina, and

$wt\%_{OTA}$ and ρ_{OTA} are weight fraction and density of OTA, and

To calculate the degree of porosity (%) of the compacted and sintered specimens the equation below is used:

$$porosity(\%) = \frac{Wsoaked - Wdry}{Wsoake - Wsuspended} \text{..................................(3)}$$

3.6.2 Thermal analysis (TGA/DTA)

TGA is used in the research to determine thermal stability and composition of various substances materials solid or liquid. In this study TGA tester which is found in Adama Science and Technology University, Material Science Department used. It is a technique that measures weight changes in a material as a function of temperature (or time) in a controlled environment. Its primary applications include determining thermal stability of a material, filler content in polymers, moisture and solvent content, and the percent composition of components in a compound. The heat flow and mass losses of the sample are monitored against temperature or time, while the temperature is programmed. The temperature was set between 25°C and 1000°C, at a heating rate of 15°C/min. TGA measures the changes in the mass loss of the sample subjected to heat under controlled atmosphere conditions.

TGA provides information about physical phenomena (phase transitions) as well as chemical phenomena (thermal decomposition). It is carried out by gradually increasing the temperature of a sample in a furnace while its weight is measured on an analytical balance that is kept outside of the furnace. If a thermal event results in the loss of a volatile component, mass loss is observed in TGA. Mass losses occur in chemical reactions such as combustion, but not in physical changes such as melting. The weight of the sample is plotted against temperature or time to show thermal transitions in the material, such as solvent and plasticizer loss in polymers, water of hydration in inorganic materials, and, finally, material decomposition. Thermal analysis of material samples will be performed to determine the exact sintering temperature in the temperature range of 23–1000°C at a heating rate of 25°C/min. It also provides degradation temperature of a material. Hence to identify our samples working temperature as thermogravimetric analysis will be performed.

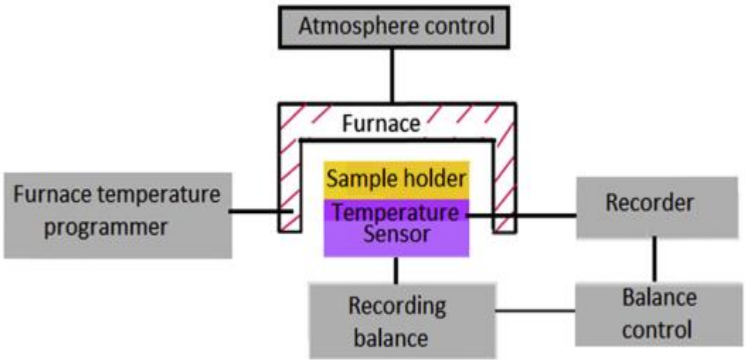

Figure 8. working principle of TGA(DTA)(Loganathan et al., 2017).

3.6.3 Phase Analysis (XRD)

XRD is a quick and non-destructive analytical technique that has mostly been used to determine the crystalline structure of olive tree ash and create hybrid composite samples. X-ray diffraction is based on constructive interference of monochromatic X-rays and a crystalline sample. A cathode ray tube produces the X-rays, which are then filtered to produce monochromatic radiation, focused by collimation, and pointed at the sample. When the circumstances are in accordance with Bragg's law ($n=2d\sin\theta$), the interaction of the incident rays with the sample results in constructive interference or destructive. This law relates the wavelength of electromagnetic radiation to the diffraction angle and the lattice spacing in a crystalline sample. These diffracted X-rays are then detected, processed and counted. By scanning the sample through a range of 2θ angles, all possible diffraction directions of the lattice should be attained due to the random orientation of the powdered material. Conversion of the diffraction peaks to d-spacings allows identification of the mineral because each mineral has a set of unique d-spacings. Typically, this is achieved by comparison of d-spacings with standard reference patterns.

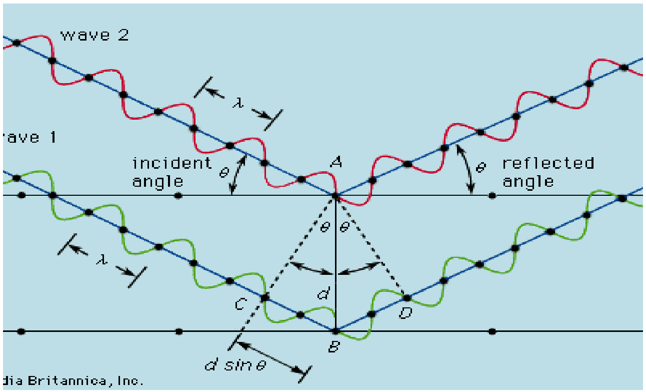

Figure 9. working principle of XRD

The XRD conducted on a fully computerized powder x-ray diffractometer (XRD-7000X-RAY DIFFRACTOMETER, SHIMADZU Corporation (Japan)) which is found in Adama Science and Technology University, Material Science Department by supplying 40 Kilo Voltage and 30 mA current and used to for phase analysis. The generated XRD spectra will be taken at an angle (2θ) ranging from 10° to 80° with a step size of 0.02°. Miller indices (hkl) are used to identify different planes of atoms and observed diffraction peaks can be related to planes of atoms to assist in analyzing the atomic structure and microstructure of a sample. When analyzing XRD data, we look for trends corresponding to directionality in the crystal structure by analyzing the miller indices of diffraction peaks. The position and intensity of peaks in a diffraction pattern are determined by the crystal structure. XRD analysis carried out on fabricated samples to determine whether any intermetallic compounds were generated during the sintering process.

To confirm the presence of the minor precipitate phases as detected by the diffraction pattern, the ‘d’ values for different phases were obtained using JCPDS cards available with the software and were manually compared with the diffraction pattern of all the samples.

3 6.4 Scanning Electron Microscopy

SEM is an instrument which is employed to observe the surface phenomena of the materials. In this study SEM| which is found in Adama Science and Technology University, Biology department used. The sample is exposed in SEM to the high-energy electron beam and gives information about topography, morphology, orientation of grains, etc. of a material. Morphology indicates the shape and size, while topography indicates the surface features of an object or “how it looks”, its texture, smoothness or roughness. In this study SEM used to study wear morphology of samples after wear test.

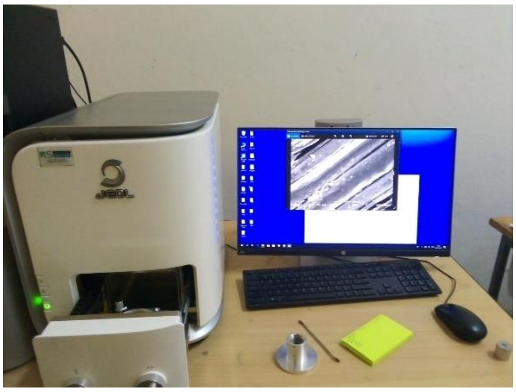

Figure 10. SEM used in this research work.

3.6.5 Vickers hardness

The material's capability to withstand scratching (abrasion) or the ability of a material to resist indentation is hardness of a material. It is defined as the material's capacity to cut different metals. It comprises other different properties such as machinability, deformation, scratching, wear resistance, etc. Hybrid composites have improved hardness, compression, and tensile strength but reduced ductility and toughness as it gets further breakable. The hardness of the composites was measured via a Vickers hardness tester machine (HVS-50) which is found in Adama science and Technology University, Material Science Department. Within the Vickers hardness test, an optical technique is used to measure the size of indentation (the diagonals) left by the indenter. The shape of the diamond tip is resembling that of a pyramid. The instrument works on the basis that an indentation is format on the polished surface at a given load. The surface area of the indent is directly proportional to the length of the diagonals of the indent formed on the surface of the sample. This measurement is then assigned a VHN. It will be experimented with under a load of 30 N for 10 sec indentation holding time, ensuring that the indentation covered an area deputy of the composite. Five trials of indentations will perform on each specimen, and lengths of the diagonals of each indentation (d_1 and d_2, average value in mm) indentation used to calculate hardness, HV according to the equation:

$$\text{Vickers Hardness(VHN)} = \frac{\text{Applied force}}{\text{Surface area of indent}} \quad \ldots\ldots\ldots\ldots\ldots\ldots\ldots\ldots\ldots (5)$$

The indent surface area can be calculated by multiplying the diagonal of the indent by a constant (0.5393). This constant is derived from the fact that the standardized angle of the pyramid face is 136°.

$$SA_{\text{pyramid}} = d^2 \; x \; \frac{1}{2 \; x \; sin\left(\frac{face\,angle}{2}\right)} = d^2 \; x \; \frac{1}{2\sin\left(\frac{136}{2}\right)} = d^2 \; x \; 0.5393 \ldots (6)$$

$$\text{VHN} = F_{(kgf)}/(d^2_{(mm)} \; x \; 0.5393) \ldots\ldots\ldots\ldots\ldots\ldots\ldots\ldots\ldots\ldots\ldots\ldots (7)$$

Where; SA surface area of pyramid

d is the length of the diagonal and

F is the force applied.

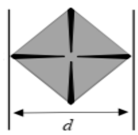

Figure 11. Schematic of Vickers indentation

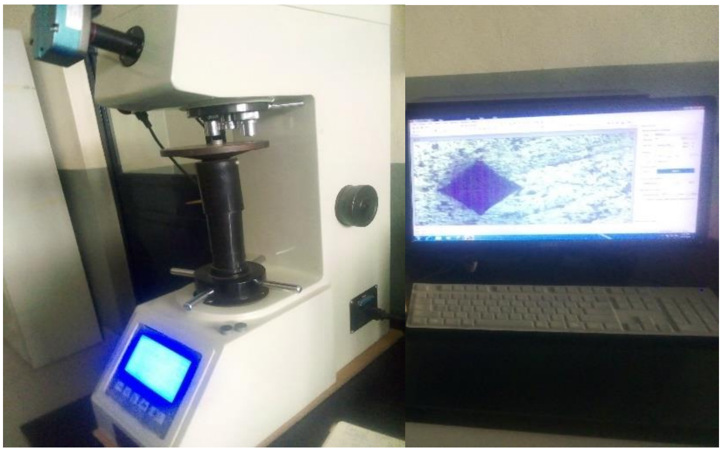

Figure 12. Vickers hardness tester used for research work

3.6.6 Compression strength testing

Compressive strength is the maximum compressive stress that under gradually applied load a given solid material will sustain without fracture. Compression strength is the capacity of a material or structure to withstand loads tending to reduce size. By definition, the ultimate compressive strength of a material is that value of uniaxial compressive stress reached when the material fails completely. The compressive strength is usually obtained experimentally by means of a compressive test, with applying of a uniaxial compressive load. In this study, the cylindrical specimens for compression test were prepared based on and then the test performed using universal testing machine (UTM) of 50KN load capacity which is found in Adama science Technology University, mechanical department. The load will apply till fracture of the specimens occur.

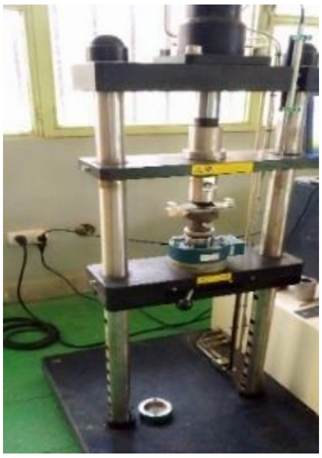

Figure 13. Universal Compression testing machine used in this study

3.6.7 Wear test

Wear is the progressive loss of material from a contact surface during relative motion between a surface and the contacting substance or substances(Shinde et al., 2020). A process of interaction in the surfaces or a face of bonded solid which is working to loss parts from solid dimension during working in its environment can be defined as a wear without or with losing of material. In the results in the wear standard tests, the removing of part from weight of the test sample can be used to expression the ear formals of the wear test. The wear rate (W.R.) is calculated using the weight or mass loss of each specimen. Equation (5) is used to compute the wear rate of the specimen using the weight technique(Omran et al., 2022).

$$WR = \frac{WL}{\pi \cdot d \cdot n \cdot t} \ldots\ldots\ldots\ldots\ldots\ldots\ldots (8)$$

Where, WR is wear rate, d is diameter of wear track of the disc, n is revolution per minute, t is time, WL is weight (or mass) loss (Weight before wear (W_b) – weight after wear (W_a)). The percentage improvement in the wear resistance of composites (IWR_{co}) compared to a base metal Al is calculated as follows.

$$IWRco\,(\%) = \frac{w_{Al} - w_{Co}}{w_{Al}} \times 100 \ldots\ldots\ldots\ldots\ldots\ldots\ldots (9)$$

Where, IWR_{co} is the percentage improvement in the wear resistance of the composite with respect to pure aluminum matrix, W_{Al} is the wear rate of pure aluminum matrix and W_{co} is the wear rate of the composite.

Pin on disk tribometer for wear analysis

Friction and wear (typically wear rates and wear resistance) characterization of materials is typically performed using various types of tribometers, while pin on disk test being probably one of the most common. The popularity of the method is due to its relative simplicity and abundance of the tribological contacts that can be well described by a simple pin on disk motion: from dry contacts of bolt screws (1) to rail wheels to rail contact (2) and to lubricated contact of biological implants. The test typically allows to test several motion modes, such as unidirectional, fretting modes and recently any other complex motion patterns. Schematically, the pin on disk test is depicted in the figure below. The stationary pin is pressed against rotating disk under the given load. The pin can be of any shape; however, the most popular shapes are spherical (ball or lens) or cylindrical due to ease of alignment of such pins (flat pins are typically subject to certain misalignment which can lead to nonuniform loading and difficulties for theoretical analysis). The wear resistance of a material depends on the interaction of asperities of the sliding surfaces. In this work, the dry sliding wear behavior of the fabricated samples investigated using pin-on disc (DUCOM TR-20 MICRO) equipment with the sample size of 6 mm diameter and 10 mm height pins dimension based on the 57 ASTM G99-05 standard. The test will be conducted at room temperature (25 °C) under the applied load of 10, 30, and 30 N with a sliding speed of 100, 200 and 300rpm on a wear track diameter of 40 mm. The friction coefficient and wear rate are considered as the main response functions for evaluating the wear performance of the composites.

Figure 14. a) Schematic of pin-on-disc tribometer used for wear test(Omran et al., 2022) b)Wear test machine used c) wear test sample

3.6.8 Potentiostat for corrosion measurement

A potentiostat is an electronic instrument that measures and controls the voltage difference between a working electrode and a reference electrode. It measures the current flow between the working and counter electrodes.

- Working Electrode – A sample of the corroding metal being tested
- Reference Electrode - An electrode with a constant electrochemical potential
- Counter Electrode - A current-carrying electrode that completes the cell circuit.

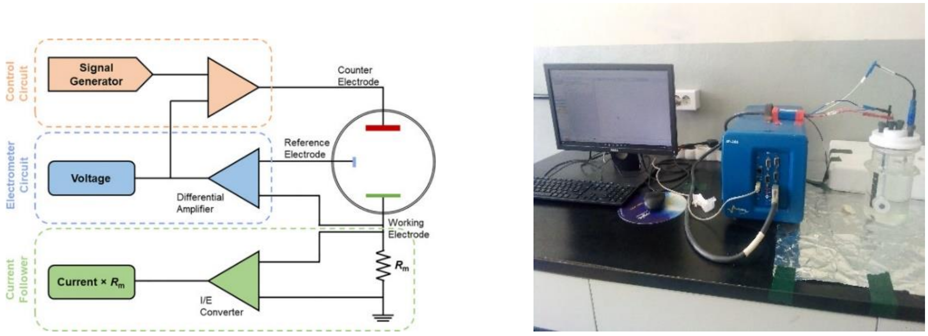

Figure 15. Basic working principle diagram left and instrument used in study right side

In potentiostatic mode, a potentiostate/galvanostatic will precisely control the capability of the C between the functioning terminal (WE) and the Reference Cathode (RE) is obvious, and compare to the worth determined by the client as should be visible from the graph, the CE is associated with the result of an electronic block which is called Control Speaker (CA). The worth of the current is estimated utilizing an Ongoing Devotee (Low CF) or a Shunt (High CR), for low and high flows, separately. The potential contrast is estimated consistently between the RE and S with a Differential Intensifier (Diff amp). Contingent upon the mode the instrument is utilized (potentiation or galvanostatic) the PSTAT/GSTAT switch is set in like manner. The sign is then taking care of into the Summation Point (Σ) which, along with the waveform set by the computerized to-simple converter (Ein) will be utilized as a contribution for the control enhancer. The cell links of the SP 300 bio rationale have a sum of five connectors: WE, CE, RE, S and ground. The potential is constantly estimated between the RE (blue) and the S (red) and the current is constantly estimated between the WE (red) and CE (dark). The ground connector (green) can be utilized to interface outer gadgets to a similar ground of the SP 300 biologic.

3.7 Taguchi based Grey Relational Analysis for Optimization of AMC process parameters

3.7.1 Taguchi Design of experiment method (DOE)

Design of experiment method (DOE) is a statistical analytic tool that helps to detect the relevant factors for the fabrication process involving planning and experimentation. Taguchi's method is the selection of control factors and t used in studying the effect of multiple variables(Sudha et al., 2019). It combines the experimental and analytical concepts to determine the most influential parameter on the result response for the significant improvement in the overall performance. It is a technique of defining and investigating all possible conditions involving multiple factors, parameters and variables in an experiment. It establishes the method for drawing inference from observation, when these observations are not exact, but subject to variations and also used to collect data(L. Singh et al., 2013).

In this method, parameters are categorized as controllable and uncontrollable. The effect of multiple parameters at two or more than two levels can be studied simultaneously using this method. There is always a target value of performance characteristic or property of any product or process.(N. Kumar & Bharti, 2022).

The four powder metallurgy process parameters, percentage of weight (OTA), compaction pressure, sintering temperature and sintering time each with three levels were selected. In this study experiment with four factors and three levels are chosen and hence orthogonal array L_{27} used. The three levels of the four parameters are shown in table below. In the run order obtained from Taguchi model L_{27} experiments were performed and the objective of this model is to obtain higher hardness value(Stalin et al., 2020).

Table 5. Process parameters and their levels

		Levels		
Process parameters	**Symbols**	**Level 1**	**Level 2**	**Level 3**
Composition of OTA	**OTA**	3	6	9
Compaction pressure (MPa)	**CP**	40	50	60
Sintering temperature(^{o}C)	**ST**	400	500	600
Sintering time(hr.)	**St**	1	2	3

Degree of Freedom (DoF) is defined as the number of comparisons made between process parameters that are made to determine a better level. It is used to compute the minimum number of experiments that will be conducted to investigate the observed factors.

Degree of freedom = number of levels – 1

Table 6. DoF at factor level

Experimental factors	**DoF (Level - 1)**	**Sub Total**
OTA	3-1	2

CP	3-1	2
ST	3-1	2
St	3-1	2
Total DoF		**8**

For this experiment L27(3^4) Orthogonal Array (OA). Where, L_{27} is the maximum number of rows or experiments. Number of levels = 3, Number of factors or columns = 4

Table 7. L_{27} (3^4) orthogonal array Experimental Design

Exp. No.	**OTA**	**CP**	**ST**	**St**
1	3	40	400	1
2	3	40	400	1
3	3	40	400	1
4	3	50	500	2
5	3	50	500	2
6	3	50	500	2
7	3	60	600	3
8	3	60	600	3
9	3	60	600	3
10	6	40	500	3
11	6	40	500	3
12	6	40	500	3
13	6	50	600	1
14	6	50	600	1
15	6	50	600	1
16	6	60	400	2
17	6	60	400	2
18	6	60	400	2
19	9	40	600	2
20	9	40	600	2
21	9	40	600	2
22	9	50	400	3
23	9	50	400	3
24	9	50	400	3
25	9	60	500	1
26	9	60	500	1
27	9	60	500	1

By transforming the results of the experiments to signal to noise ratio the deviation of quality characteristic can be measured. The high value of the SN ratio implies that the value of the signal is high, and the value of the noise is low. So, the parameter levels, which give the maximum values of the SN ratio, are the optimum parameters(N. Kumar & Bharti, 2022).

The three statistical formulas for calculating SN ratios(Ravichandran et al., 2015)

Smaller is better S/N = -10 log $\frac{1}{3}\sum_{i=1}^{3} y_i^2$, responses like porosity experimental density

Large is better S/N = -10 log $\frac{1}{3}\sum_{i=1}^{3}\frac{1}{y_i^2}$, responses like hardness and compressive strength

Nominal is better S/R = 10 log$\frac{\mu^2}{\sigma^2}$, S/N on means and standard deviations

3.7.2 Grey relational analysis

Grey Relational Analysis (GRA) is an efficient tool for multi-response analysis. GRA is a measurement of the absolute value of the data difference between sequences, and it could be used to measure the approximate correlation between sequences.

This study aimed: - (1) to minimize Porosity and experimental density

(2) to maximize micro-hardness and compressive strength of AMC via PM. Multiple input parameters are weight percent of OTA, Compacting pressure, Sintering temperature and sintering time. Responses considered are density, porosity, hardness and compressive strength.

Grey Relation Grade (GRG) is used to determine the most influential combination of parameters. It also used to identify the most significant levels of input parameters to obtain improved results.

Steps of GRG used for optimization are shown below.

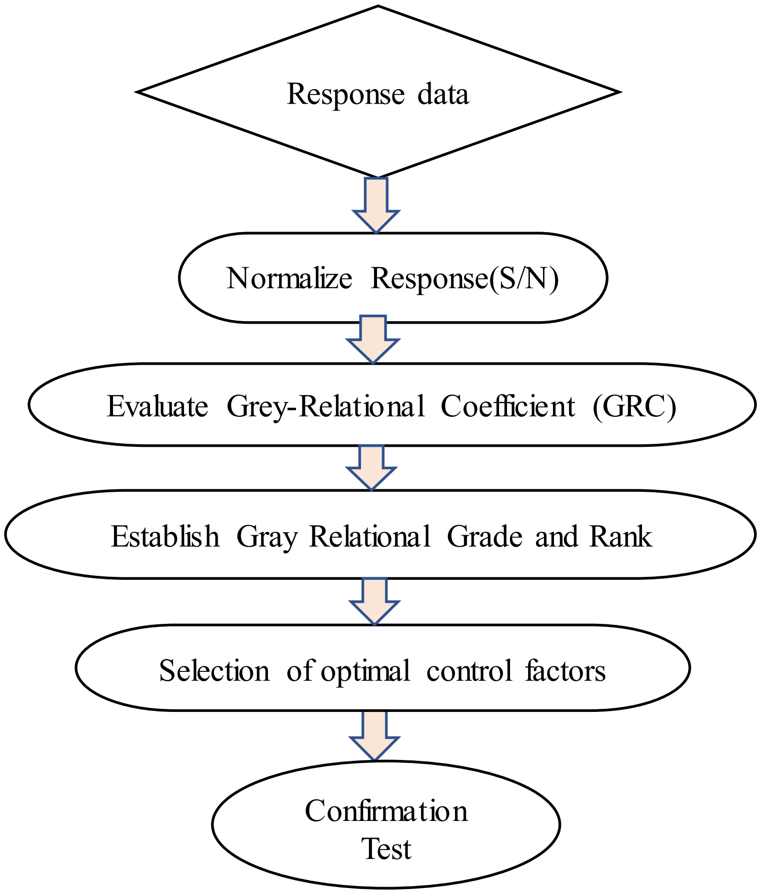

Figure 16. Major steps in Taguchi GRA

3.8 Equipment's used throughout the study

Table 8.Tools and Equipment utilized in the study, including its type and function

Equipment	Location	Function
High energy ball mill	ASTU	➲ Blending or mixing and grinding into a very fine powder of the Al matrix and the Mg, Gr, and OTA particulate reinforcements.
Hydraulic pressing machine	ASTU	➲ The blended Al- (Mg + Gr + OTA) hybrid composite powder forming a green compact body.

Electrical muffle furnace	ASTU	➲ Sintering the hybrid composite specimens that were green-compacted, at a specific temperature to increase strength and density. ➲ To calcinate OTA and produce fine powder for reinforcement in the manufacturing of hybrid composites.
Grinder/Polisher	ASTU	➲ To produce a smooth, scratch-free mirror-like surface for hardness and optical microscope.
Optical microscope (OM)	ASTU	➲ For examining the micro structural characteristics of the prepared composite sample.
Scanning Electron Microscope (SEM)	ASTU	➲ To understand the wear mechanism of unreinforced Al matrix and hybrid composite specimens. ➲ To investigate how surfaces are affected by corrosion.
Thermogravimetric Analysis (TGA/DTA)	ASTU	➲ To determine calcination temperature olive tree powder and check its stable temperature. ➲ To perform thermal analysis and determine the exact sintering temperature in the temperature range from room temperature up to 1000°C at a heating rate of 25°C/min. ➲ To determine working temperature of produced composite samples
X-ray diffraction (XRD)	ASTU	➲ Determine the relative amounts of phases in a mixture by using the relative peak intensities while analyzing the quantitative phase composition of a sample.
Fourier Transform Infrared Ray (FTIR)	Bahirdar University	➲ For interfacial reaction and functional group study of the OTA ash and Composite materials

X-ray Fluorescent (XRF)	Ethio-Geological Survey	➲ For compositional analysis of OTA
Vickers hardness machine	ASTU HV50	➲ To test the hardness of the matrix and composite
Universal test machine (UTM)	ASTU	➲ To test the compressive strength or capacity of prepared composite sample
Pin-on-disc test apparatus	AASTU (DUCOM TR-20 MICRO)	➲ Used to investigate the wear rate and coefficient of friction of the hybrid composite samples
Electronic weighing machine	ASTU	➲ For measuring the weight of powder, sample for density and porosity, and loss of the specimens during the wear test.
Electrical oven	ASTU	➲ For drying the OTA sample after proper washing

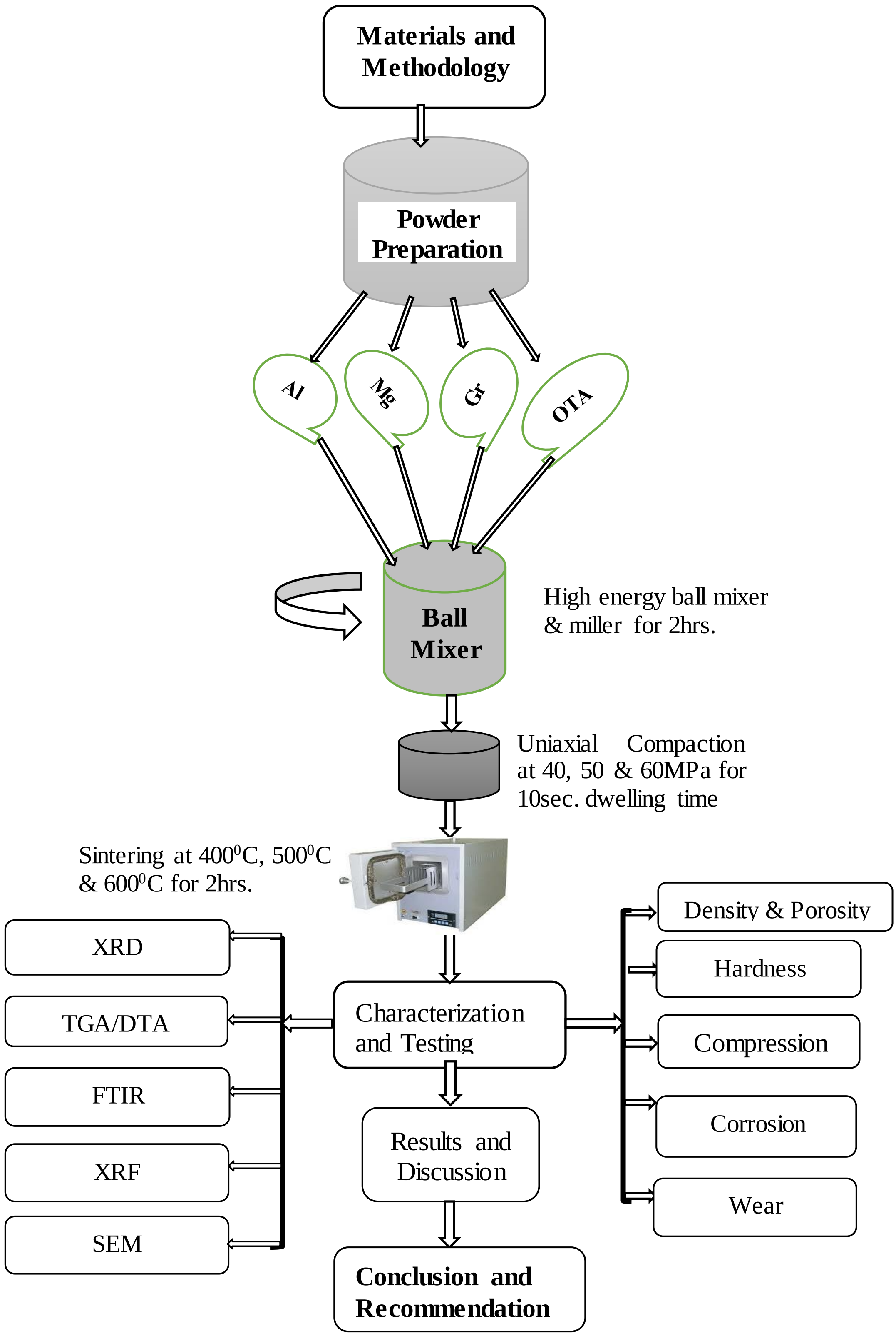

Figure 17. Flow chart of overall process showing research methodology.

CHAPTER FOUR

RESULTS AND DISCUSSION

4.1 Thermal Analysis Result of Olive Tree Stem Powder.

The thermal performance of the powder can be measured using the TGA method as the material's weight changes. While keeping a steady heating rate, the physical attributes can be measured as a function of temperature rise. A thermal analyzer measured the mass losses. The TGA and DTG curves in Figure 16 below were used to analyze the thermal stability of olive tree stem powder. Olive tree stem powder weighing 12.048 mg was put in a crucible and burned under nitrogen flow for 50 milliseconds. A heating rate of 10 °C/min was used with a temperature range of 25 °C and 900 °C. TGA examines the variations in the sample's mass loss after being heated in a controlled atmosphere.

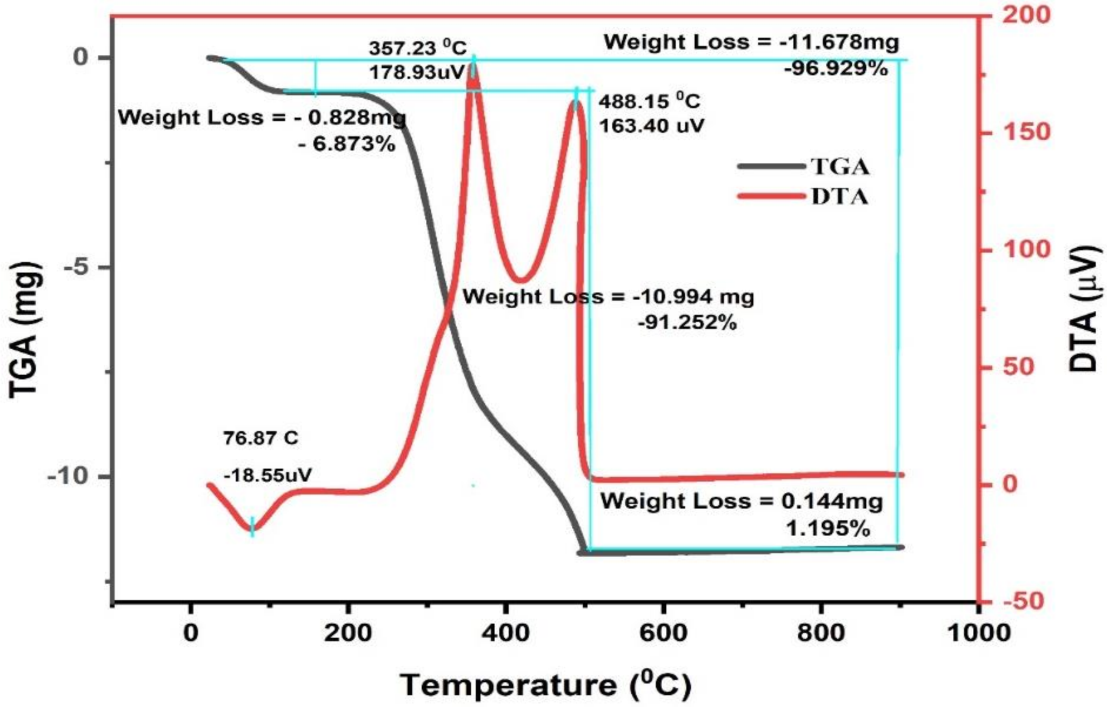

Figure 18. TGA/DTA results of olive tree stem powder

In the first step, degradation started at around 357.23°C (between 50°C and 357.23°C) and weight loss of 0.828mg (6.873%). This weight loss revealed the evaporation of the moisture and volatile material present in the powder. The second degradation occurred between 357.23°C and 488.15°C with a weight loss of 10.994mg. This degradation was due to the degradation of hemicellulose, lignin, and others(Alshammari et al., 2019b). The third and final stage of weight loss occurred at 488.15°C with a weight loss of 0.144mg (1.195%) and corresponds to the elimination of α-cellulose and lignin content from the powder. The decomposition of lignin is extended up to 600°C. Based on the thermal result a temperature of 600°C and above can be chosen for calcination because it a stable stage range. Because all moisture, hemicellulose, and lignin are decomposed above 600°C. Hence, olive tree stem powder was calcined at 850°C for 2hrs to remove all unnecessary materials and to obtain SiO_2, Al_2O_3 and others important for reinforcement.

4.2 Compositional and Phase Analysis OTA Particulates

Table 9. XRF analysis of OTA particulates

Chemical composition	SiO_2	Al_2O_3	Fe_2O_3	CaO	MgO	Na_2O	K_2O	MnO	P_2O_5	Tio_2	H_2O	LOI
Amount (%)	17.74	6.63	3.24	11.50	0.96	2.20	4.50	1.38	1.25	0.07	0.89	49.73

From the above table data, sample OTA has the largest composition of primary components (SiO_2+Al_2O_3+Fe_2O_3+CaO), which is 39.11%. The result was minimum when compared with other solid agro-waste like bamboo, baggash ash, rise husk, and coconut ash. Also, there were other chemicals not identified by XRD. It may be due to thermal effect on ash and their amount. In general, the existence of required hard ceramic oxides confirmed.

4.3 XRD results olive tree

XRD is a rapid and non-destructive analytical technique that has been used primarily to identify the crystallographic structure of the olive tree stem powder calcined at 850°C for 2hrs. Figure 17 below shows the XRD patterns of the powder. XRD-7000X-Ray Diffractometer Shimadzu Corporation (Japan) which is found in ASTU materials engineering, is used in this study. It revealed the main reflection peaks at 2θ =22.14°, 26.6° and 29.5°. Peaks at 2θ=22.14° and 26.6° are verified the existence of SiO_2 (JCPDS card number 00-046-1045). Peak at 2θ=29.5° depicted the existence of calcite. Hence OTA used as reinforcement(filler) due to existence of hard calcined oxides.

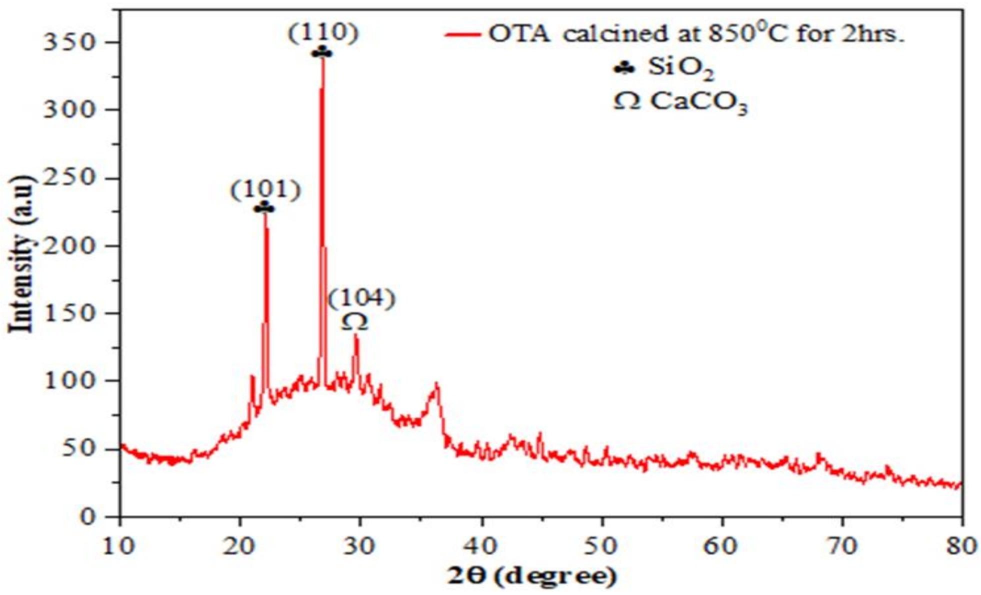

Figure 19. XRD results of Olive Tree stem ash particle after calcination

4.4 Thermal analysis of AMC samples

Figure 20 below the TGA/DTA curve of four samples A0OTA, A3OTA, A6OTA and A9OTA shown. At the beginning 23.27° the curve represents 100% wt.% for A0OTA in Figure 20(a). From 27.61°C - 33.31°C no weight loss or gain observed. But slight weight loss of material observed at 33.31°C – 192.08°C(0.01mg). This is supposed to be loss(removal) of moisture and volatile materials. when heating continued from 192.08°C-245.33°C no weight gain or loss observed. But from 245.33°C-280.92°C (0.01mg) of weight gain observed. It is supposed to be oxidation of aluminum in presence of impurities in aluminum and oxygen in nitrogen environment(Bell et al., 2006). This weight gains also continued from 281.06°C up to 317.61°C with constant mass gain of 0.02mg. Similarly, from 318.00°C -350.05°C, 350.03°C-380.31°C, 380.43°C-406.89, 407.89°C-430.61 and 430.93°C-455.36°C weight gain of 0.03mg, 0.04mg, 0.05mg, 0.06mg and 0.07mg respectively observed. At 661.21°C(-20.80uV) exothermic peak (phase change) observed since it is the melting temperature of aluminum. Another endothermic peak also revealed at 681°C(12.40uV) due to phase change. Weight gain continued up to 1000°C. It is also supposed to be oxidation of aluminum, since the temperature is above melting temperature of aluminum Here the thermal effect on matrix and secondary reinforcements observed. Magnesium normally wets at temperatures between 500°C and 600°C in an aluminum matrix, which is a comparatively low temperature. The aluminum matrix starts to soften at these temperatures, which can aid in wetting and bonding between the magnesium and aluminum(Sangghaleh & Halali, 2009). Intermetallic compounds that form at the interface of magnesium and aluminum can also serve to improve the wetting behavior, increase the strength, and lengthen the lifespan of the resulting composite material. Total weight loss at 1000°C was 1.623mg (26.650%). This is higher when compared with other OTA reinforced samples.

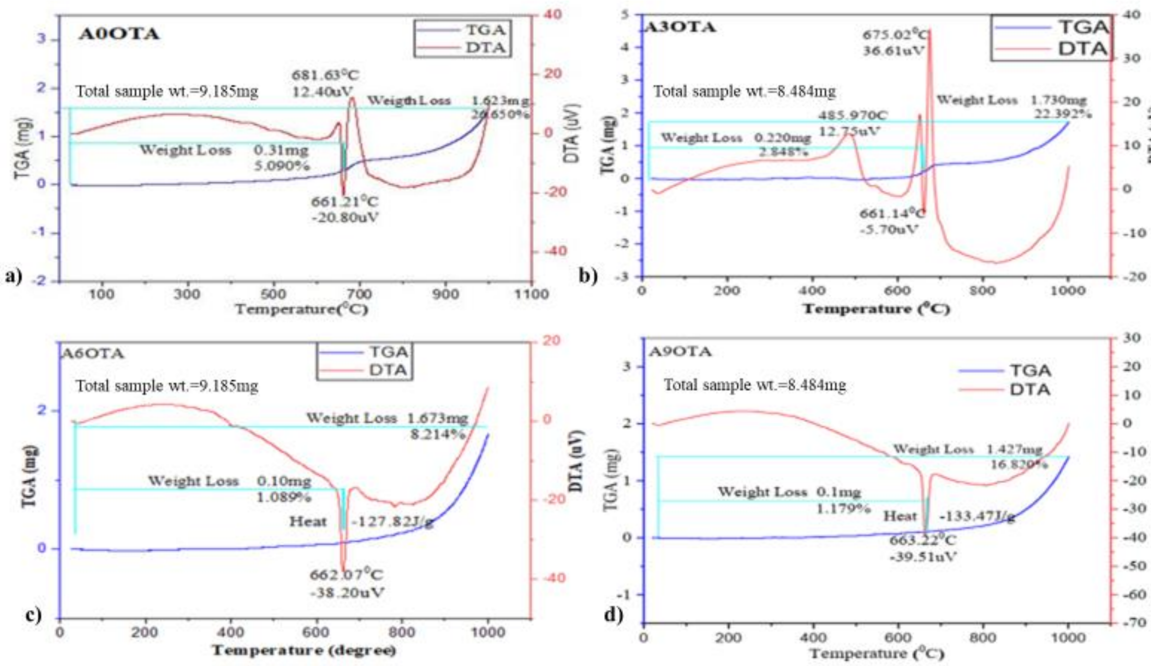

Figure 20. TGA/DTA graph of (a) A0OTA (b) A3OTA (c) A6OTA and (d) A9OTA.

In figure 20 above (b) – (d) the TGA/DTA represented for A3OTA, A6OTA and A9OTA respectively. They were with additives (Gr and Mg) and reinforcement (OTA). In A3OTA(b) 23.29°C-56.39°C exothermic reaction and 56.77°C-305.14°C endothermic reaction indicated. Weight loss started from 23.29 and continued to 305.14°C. In this curve the effect of OTA addition on thermal stability and phase change was shown. Here weight loss started earlier than A0OTA. It is supposed that OTA has high moisture absorbance capability, hence more moisture content than previous sample. Weight loss started from 37.37°C and continued up to 305.14°C with its increasing energy absorbance (endothermically). But for short period material was stable (305.14°C-307.42°C). Then wait gain proceeded up to 332.86°C and again after short stable interval proceeded mass loss up to 341.12°C. Long stable range observed from 341.5°C - 369.93°C. These stable ranges are assumed to be that the oxide layer produced from magnesium and base material during reaction are straggling to resist heat and degradation. From 370.25°C - 458.66°C weight loss due to endothermic process. At 485.9°C, 651.91°C, and 675.02°C endothermic peak, and at

661.14^{o}C(-5.7uV) exothermic peaks depict that there was phase change. A3OTA has higher thermal stability than A0OTA due to incorporation of OTA, from 53.92^{o}C-275.8^{o}C slight weight loss involved.

Figure 20(c) represent A6OTA. In the stage from 27.42^{o}C to 53.9^{o}C no any weight gain or loss observed. But there was a small energy absorption. Then moisture or volatile impurity loss started at 53.59^{o}C and lasted at 275.8. Then material was stable from 276.1-400.77^{o}C. Due to increment of OTA from 3wt.% to 6wt.%, hence thermal stability range of this sample increased. It has high thermal stability than A0OTA. And, it has one exothermic peak at 662.07^{o}C (0.10mg mass gain). It was higher than that of A0OTA which was (0.22mg) at 661.14^{o}C. As the temperature increases from 662.07 to 1000^{o}C weight gain increases due oxidation and the oxide layer thickness increases, and further decomposition (degradation) of material not observed. When compared to A0OTA and A3OTA, A6OTA has long stable range and less weight loss and gain observed as it depicted above in figure 20(a), (b) and (c).

The fourth sample, as in figure 20(d) shown, has only one peak at 663.22^{o}C which was an exothermic(-39.51uV) with mas gain of 0.1mg. Mass gain continued up 1000^{o}C. This indicates oxidation of the material increases as temperature increases. Uniform slight mass loss observed from37.37^{o}C-281.11^{o}C, due to moisture and impurity evaporation. From 281.41^{o}C to 379.73^{o}C material was stable. It has least total mass loss compare to all other samples, that is 1.427mg (16.82%).

In general, all samples experienced heat absorbance with weight gain in first stage, then wait gain for some interval and for some interval stable. Almost in all samples an exothermic peak observed at the melting point of aluminum, due to phase change. Since the melting point of aluminum is 660^{o}C, it starts to soften and as heating continues it melts(fuse) leaving Gr. and OTA in the system. Also, magnesium has melting point 650^{o}C, it also melts(fuse) together with aluminum. Samples in figure 20(b), (c) and (d) are stable from 300^{o}C to 610^{o}C except sample (a). Based on TGA/DTA result, phase transformation temperature for A0OTA (661.21), A3OTA (661.14^{o}C), A6OTA (662.07^{o}C) and A9OTA (663.22^{o}C) occurred. Hence the sintering temperature of composite must be between 0.7% - 0.9% of the phase transformation temperature of the material, also the result supported. Based on this the sintering temperature of the composite material (400^{o}C, 500^{o}C, and 600^{o}C) were selected.

4.5 XRD result of OTA reinforced AMC

XRD patterns of the AMC samples were drawn below by using Origin software. Figure 21(a) XRD plot AMC before sintering as mixed or milled. In this graph aluminium peaks are observed and peaks from other material were dominated by aluminium, since it has highest composition has high(Saini et al., 2022) intensity. Based on graph no any undesirable materials formed during milling the composite powder. But when the composition of OTA increases very small peaks were emerged indicating the existence of siO_2, Gr and Mg. The intensity of SiO_2 in OTA was very small compared to aluminium peak, hence other peaks were dominated by base material. But very small peaks from SiO_2 observed at =26.61° (JCPDS card number :00-046-1045) corresponding to (110). Also, minor peak of Gr. was shown at 2θ=26.614(111) and (JCPDS card number: 025-0284).

After sintering as indicated in figure 21(b), (c) and (d) below no such much difference observed. Formation of no new material revealed. Aluminium peaks are dominated all others peaks.

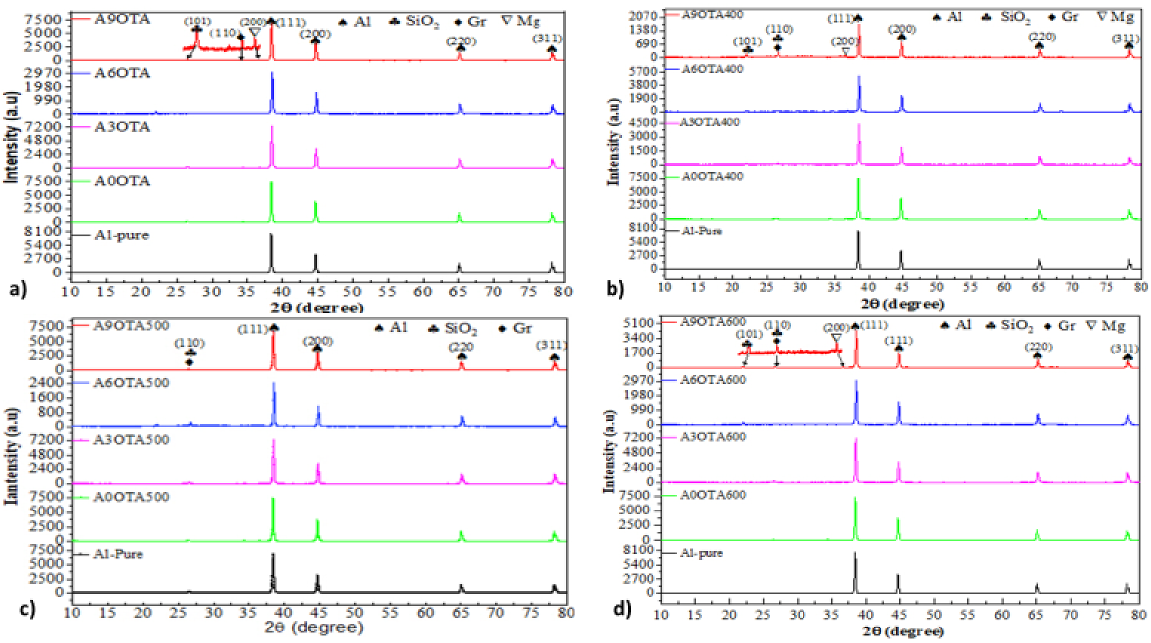

Figure 21. XRD results of AMCs of (a) before sintering (b) sintered at 400^0C (c) sintered at 500^0C (d) sintered at 600^0C

4.6 FTIR of samples sintered 600^{0}C

Fourier transforms infrared spectroscopy (FTIR) of the samples was conducted in the range of wavenumber 4000–500 cm^{-1} using infrared spectrometer. The vibration of the main functional groups of Si-O and Al-O observed from the range between 500-1000cm^{-1}. The band at around 914, 540, and 470cm^{-1} regards to Si-O-Si bending vibration. These bands were assighned to the symmetric and asymmetric vibration of valence bonds Si-O-Si(Saini et al., 2022).

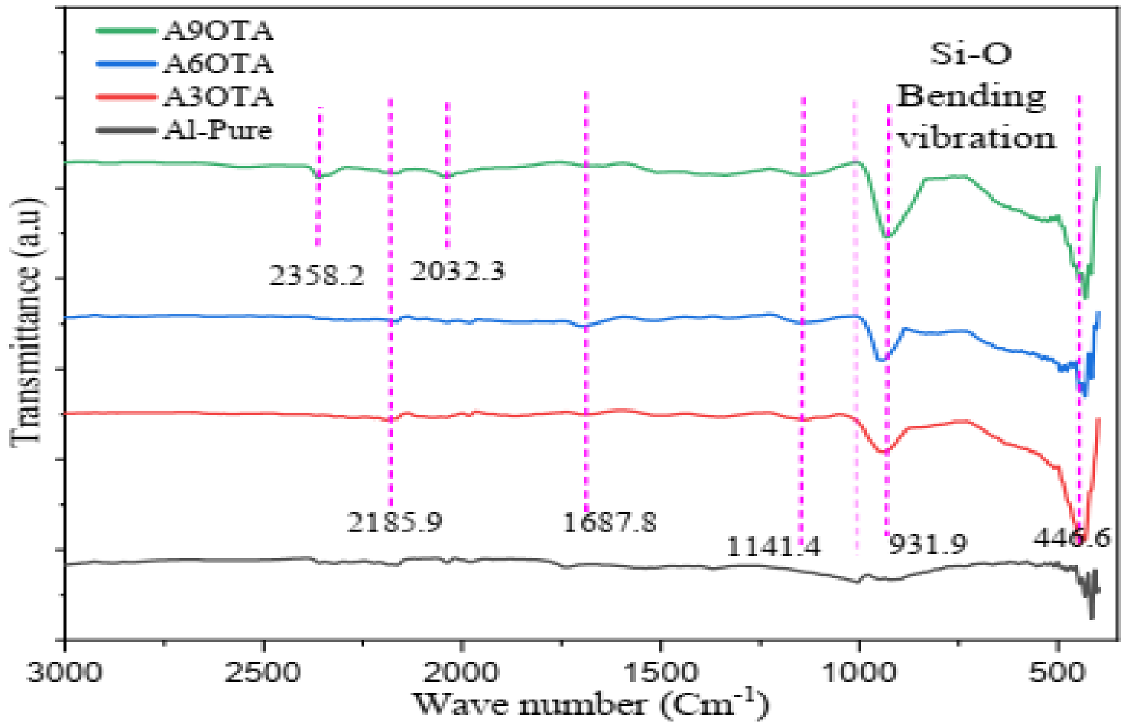

Figure 22. FTIR spectra of the AMC samples sintered at 600^{0}C

4.7 Physio-mechanical Behaviour of AMCs

4.7.1 Analysis of density and porosity measurement

Density and porosity tests are the main physical tests done on AMCs. Calculating density involves applying the Archimedes principle. Typically, the obtained samples are weighed both in dry (air) and in water, a liquid with known density. Porosity is a measure of the amount of void space between powder particles, as opposed to density, that is the ratio of mass to total volume of a composite material. It observed that the theoretically derived density values are lower than base(matrix) material for all samples. As the composition of

OTA increases A0OTA to A9OTA the both the theoretical and experimental density decreases since low density.

This is due to the low density of OTA which is less than base material and additives Gr ($2.28g/cm^3$ and magnesium ($1.74g/cm^3$). As the composition of OTA increases the porosity increases but showed small change in A3OTA400, A6OTA500 and A9OTA600 as their results indicated below in the table. In addition to that also they experienced enhanced hardness, strength, wear resistance and corrosion as (Orhadahwe et al., 2020). This is due to optimum compatibility of processing parameters (Seshappa & Anjaneya Prasad, 2021). The increased composition of composition of OTA, insufficient compacting pressure(40MPa) and Gr. (3wt%) increased porosity which facilitate (initiate) cracking in composites, and the Gr. Amount above the optimum value could also cause porosity because of its light weight and inability to easily rearrange and move with the Al, instead accumulating in some portions, causing partial distribution of hybrid reinforcements in the Al matrix. In the table 10 below experimental, theoretical and porosity of composite specimens sintered at 400^0C, 500^0C and 600^0C respectively were shown. In all case as the weight percent of OTA increases experimental the density decreases and porosity also increases up to 3wt.%, and 6wt.% point respectively then decreased.

Table 10. Density and porosity of the composite specimen sintered at 400^0C for 2hrs.

Sample Design	**Exp. Density (g/cm^3**	**Theo. Density ($g/cm^{3)}$**	**Porosity (%)**
Al	2.612	2.7	2.184
A0OTA	2.563	2.663	4.011
A3OTA	**2.522**	**2.61**	**3.827**
A6OTA	2.490	2.557	3.994
A9OTA	2.418	2.504	4.499

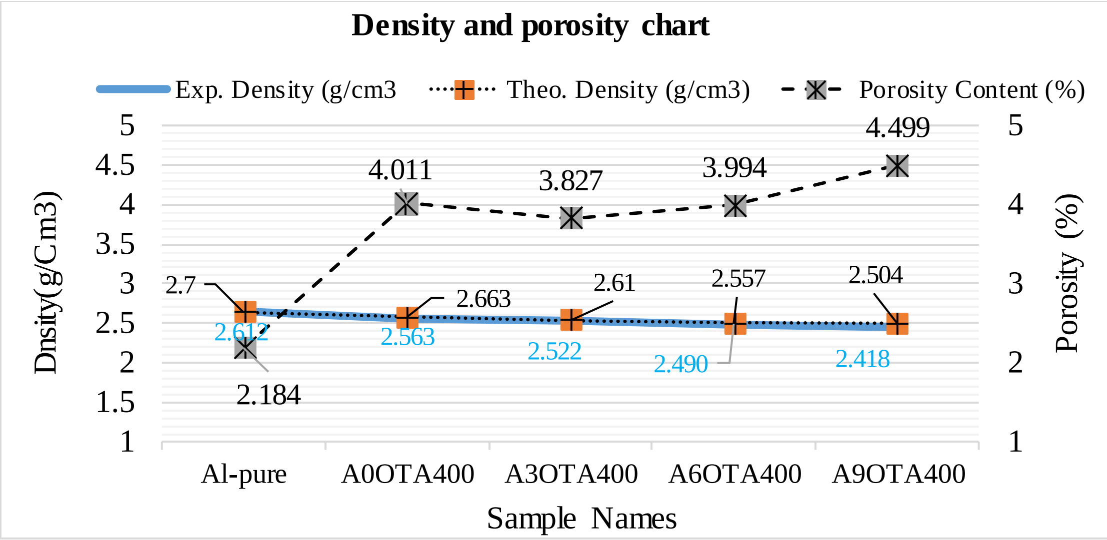

Figure 23. Density and porosity of specimens sintered at 400^{0}C

From the above table 10 A3OTA400 has lowest porosity when compared with other composite samples. Since the sintering temperature was minimum as OTA composition increases porosity increased due to less binding force between particles. A3OTA has less porosity due less OTA composition hence optimum temperature for better consolidation of particles.

Table below shows the variation of experimental density, theoretical density, and % porosity content with the different compositions of the AMC second batch specimen.

Table 11. Density and porosity of the composite specimen sintered at 500^{0}C for 2hrs

Sample Design	Exp. Density(g/cm3)	Theo. Density	Porosity (%)
Al	2.628	2.7	2.021
A0OTA	2.560	2.663	2.636
A3OTA	2.523	2.61	3.470
A6OTA	**2.517**	**2.557**	**3.245**
A9OTA	2.456	2.504	3.645

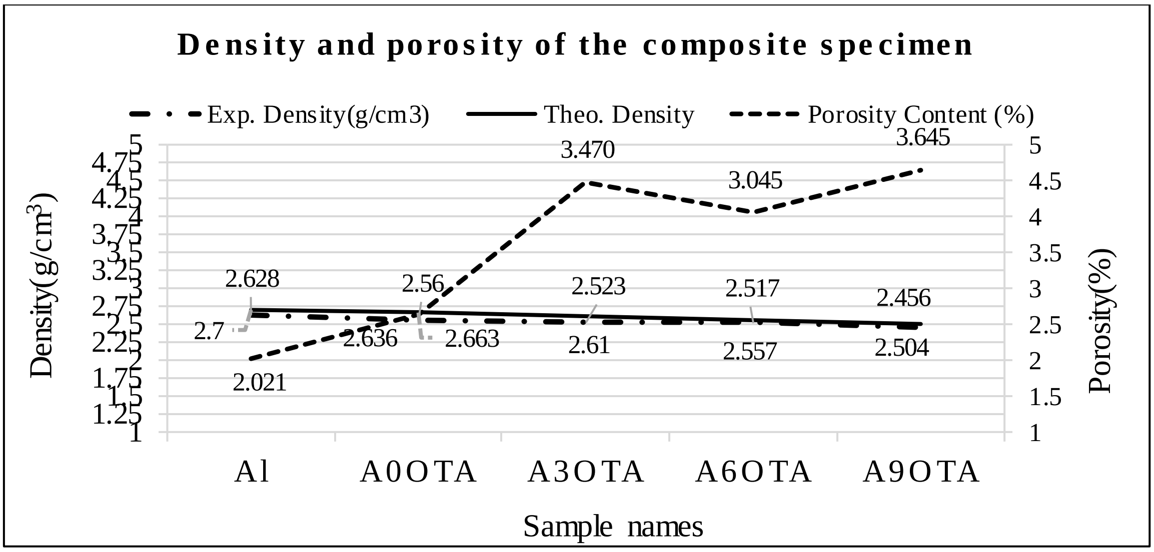

Figure 24. Experimental and theoretical density with porosity of sample.

From this batch sample with 6wt.% of OTA had least porosity with optimum density. When we compare with first batch sample this batch the sintering temperature increased to 500^0c. Minimum porosity was contained in sample with 6wt.% of OTA. This indicates that increase in sintering temperature resulted minimum porosity even if OTA wt.% increases.

Table 12. Weight and bulk density of the composite specimen at various stages (sintered at 600^0C for 2hrs)

Sample Design	Exp. Density	Theo. Density	Porosity (%)
Al	2.668	2.7	2.739
A0OTA	2.58	2.66	2.861
A3OTA	2.512	2.61	3.210
A6OTA	2.372	2.557	3.359
A9OTA	**2.314**	**2.504**	**3.195**

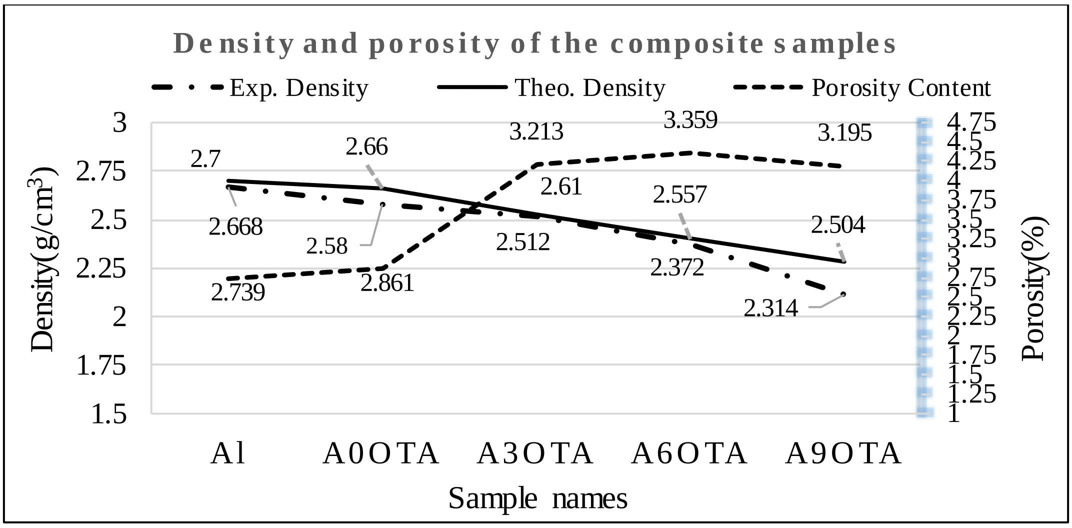

Figure 25. Experimental and theoretical density with porosity of sample.

In this batch sample the sintering temperature increased to 600^0C. The sample with minimum porosity was with 9wt.%.OTA. The increase in temperature resulted minimum porosity. This also supported by the optimization result that the sintering temperature was most influencing factor next to compacting temperature. High temperature facilitates diffusion, hence increase density and mechanical property. When compared with all other samples, A9OTA had the least porosity

4.7.2 Vickers Hardness

The hardness tests were performed using a Vickers hardness (HVS50) testing equipment in accordance with 30 kg of load for a 10 seconds dwell time. Before the test was conducted, the samples were grinded and polished to create a smooth, plane surface easily to differentiate indented surface of samples. The test was conducted at room temperature (27°C), and each sample's hardness measured on five distinct places to get an average hardness result. The five trials changed into average values are recorded as shown below in the Table 16. The result indicates that the addition of 3 wt.% OTA improved to the maximum value (39%) from samples sintered at 400^0C and addition of 6wt% OTA improved maximum value (43.6%) from the samples sintered at 500^0C. Similarly, addition of 9wt% OTA improved maximum value (54.2%) from all other samples sintered at 600^0C when compared to pure matrix metal and they have highest hardness value. From the all batch sample three with 9wt.% OTA has highest improvement (54.2%). It has been observed that reinforcement wt % have a higher impact on density and porosity than sintering temperature as(Composites, 2022). Based on hardness value the third batch sample

(A9OTA600) has high enhancement. This is due to high sintering temperature reduce porosity and increase density.

The percentage of improvement is calculated as

$$\text{Improvement } (\%) = \frac{x_i - x_i^0}{x_i^0} \times 100 \ldots\ldots\ldots\ldots\ldots\ldots\ldots\ldots \text{(10)}$$

Where, x_i is the average (HV and CS) value of AMC and x_i^0 is base metal matrix Al. All improvement calculations are based above equation throughout research.

Table 13. Average hardness of three batch samples sintered at 400^0C, 500^0C and 600^0C

Samples	**Average HV (sintered at 400^0C)**	**Average HV (sintered at 500^0C)**	**Average HV (sintered at 600^0C)**
Al	155.66	174.1	172.08
A0OTA	158.82	209.74	214.74
A3OTA	**215.4**	238.02	241.30
A6OTA	212.24	**249.96**	250.96
A9OTA	185.24	217.08	**265.26**

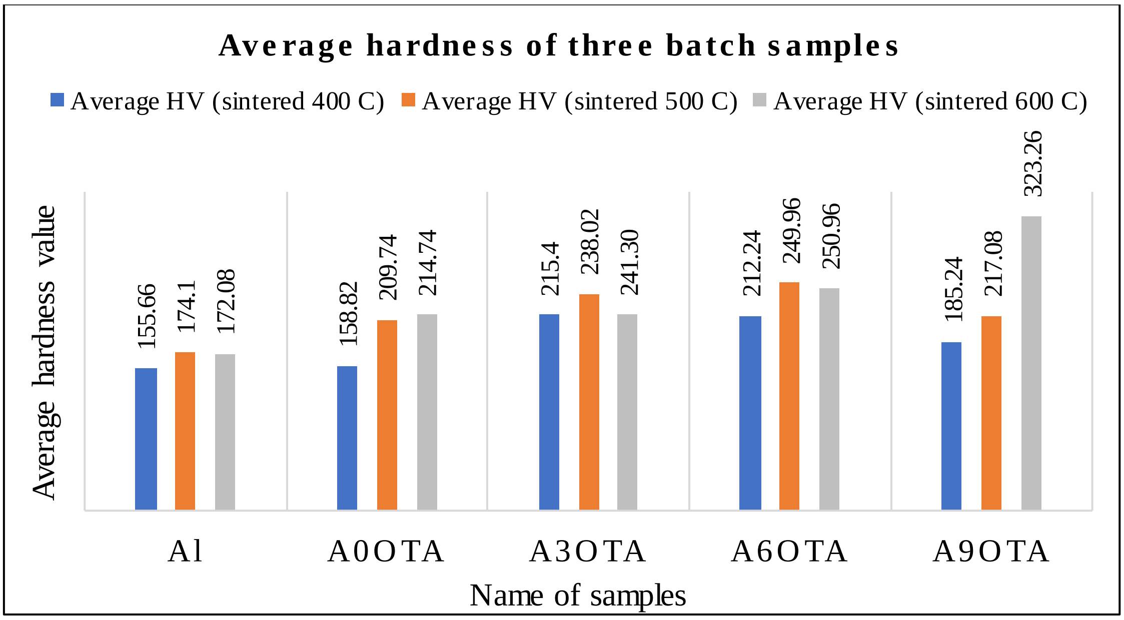

Figure 26. Bar graph of Average hardness of three batch samples

4.7.3 Compressive strength testing

Based on the results below in the table 17 the compressive strength of composite enhanced due to incorporation of OTA with additives and optimum sintering temperature. The addition of reinforcements into base metal during processing enhanced the compressive strength as shown below in the table. As indicated values in the table all reinforced samples showed improvement. From the first batch 3wt.% OTA has highest value of improvement (47.6%) in its batch. From second batch, 6wt.% OTA has highest improvement (43.6%) in its batch. From the third 9wt.% OTA has improvement value (52.5%) in its batch. When all are compared, the third batch with 9wt.% OTA has highest value (52.5%). This result is also supported by above hardness value. It also supposed to that Mg facilitated good wettability for good bonding. The microstructure formed act as barrier to grain dislocation. As the addition of OTA increases compressive strength enhanced.

Table 14. Average compressive strength of three batch samples

Samples	**Average CS (400^0C) MPa**	**Average CS (500^0C) MPa**	**Average CS (600^0C) MPa**
Al	144.435	149.012	148.65
A0OTA	158.027	168.447	190.841
A3OTA	**213.159**	215.527	219.986
A6OTA	209.581	**224.045**	221.229
A9OTA	211.904	219.334	**226.742**

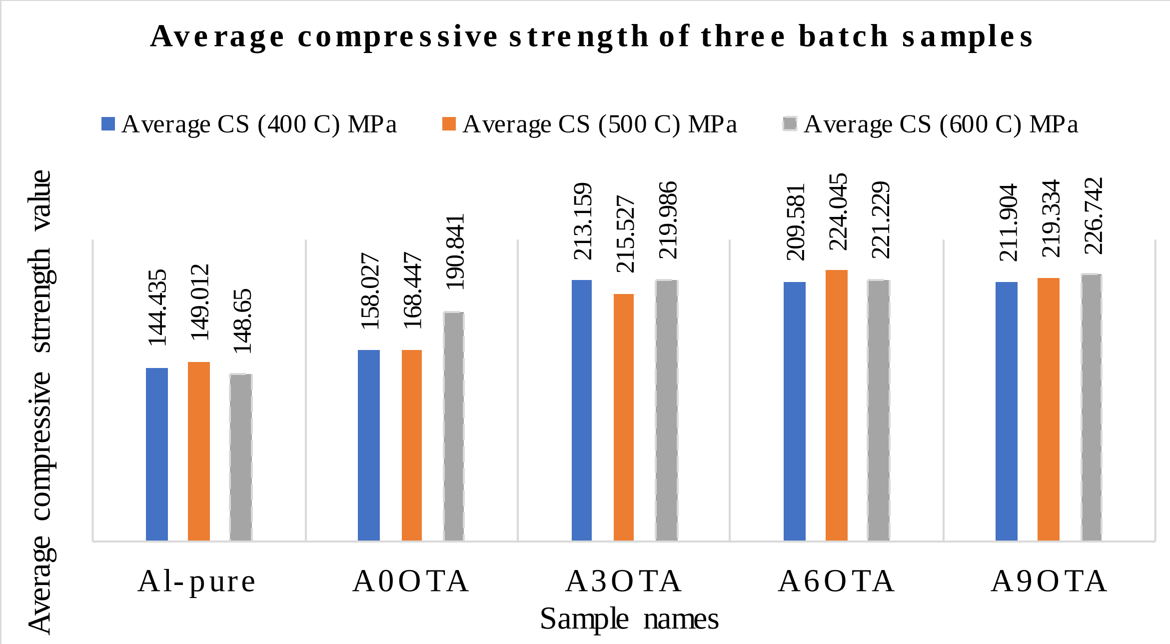

Figure 27 Average compressive strength of three batch samples

4.8 Tribological Behaviour of AMCs

4.8.1 Dry sliding wear Behavior of AMCs

When a surface moves relative to the contacting substance or substances, wear occurs, which is the gradual loss of material from the contact surface. Wear without or with material loss may be defined as a process of contact in the surfaces or a face of bonded solid that is working to lose portions from dimensions solid while working in its environment. As it is plotted on the graph below wear loss versus load for a base Al and three Al/Gr/ mg/OTA with varying composition of OTA particulates. The main element affecting AMC wear during sliding is the applied load. According to figure 28 blow, the wear loss of base metal and AMCs increases as applied load increases. With a higher load, the wear rate rises significantly because of the increased contact pressure, which has consequences like removing the softened matrix phase and fragments of broken reinforcing particles, which stimulates abrasive wear(Téllez-Villaseñor et al., 2021). In practice, oxidative or mild wear happens when applied loads are below this threshold value, and metallic or severe wear happens when applied stresses are higher, which is followed by increased plastic deformation. When the load is increased from 10 to 30 N, the wear loss of Al rises. The wear degrading at higher loads cause the increase in wear loss. When sliding wear occurs, the temperature of Al increases, causing significant damage.

The hardness, as well as the sharpness of a material's surface influence its wear resistance. These improved properties boost the AMAC's resistance to plastic deformation at the subsurface and its wear resistance.

Wear loss in AMCs reduces with the addition of additives (3wt%. Gr) and increasing amount of OTA up to its optimum amount 6wt.%OTA as indicated figure 28 below. In this work, the dry sliding wear behavior of the samples fabricated were investigated using pin-on disc (DUCOM TR-20 MICRO) equipment with the sample size of 6mm diameter and 12mm height based on the ASTM G99-05 standard. By comparing the weights of each specimen before and after the wear test, the wear mass loss of each specimen was measured.

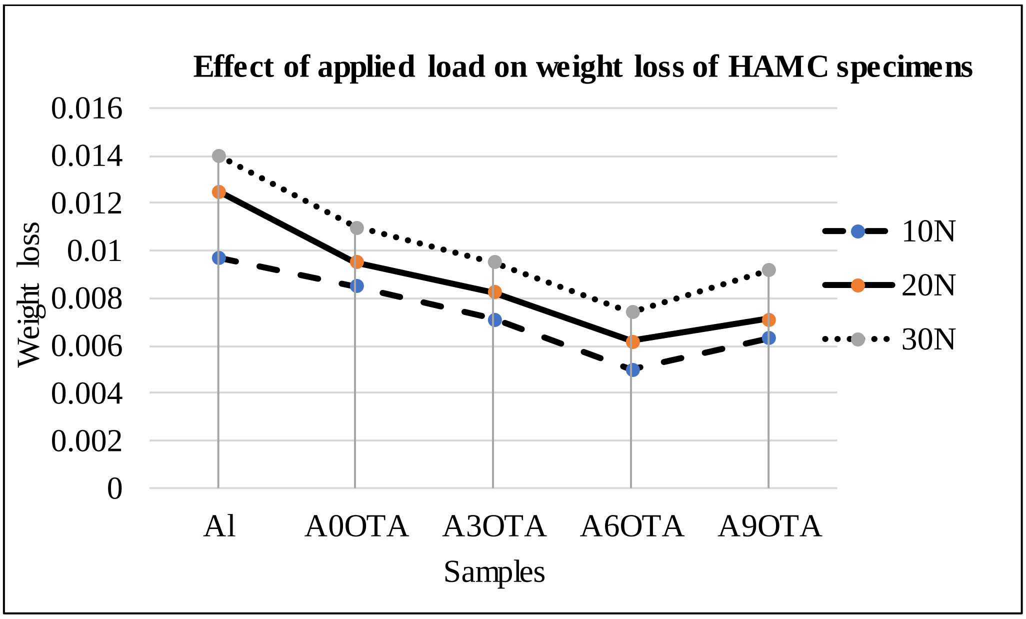

Figure 28. Effect of applied load on weight loss of HAMC specimens

From the figure as the wt.% OTA increases up to 6%, there was reduction in weight loss. This is supposed to be that as more OTA introduced, more hard particles from the ash increase the hardness of the composite (hardness =249.96 for 6%OTA).

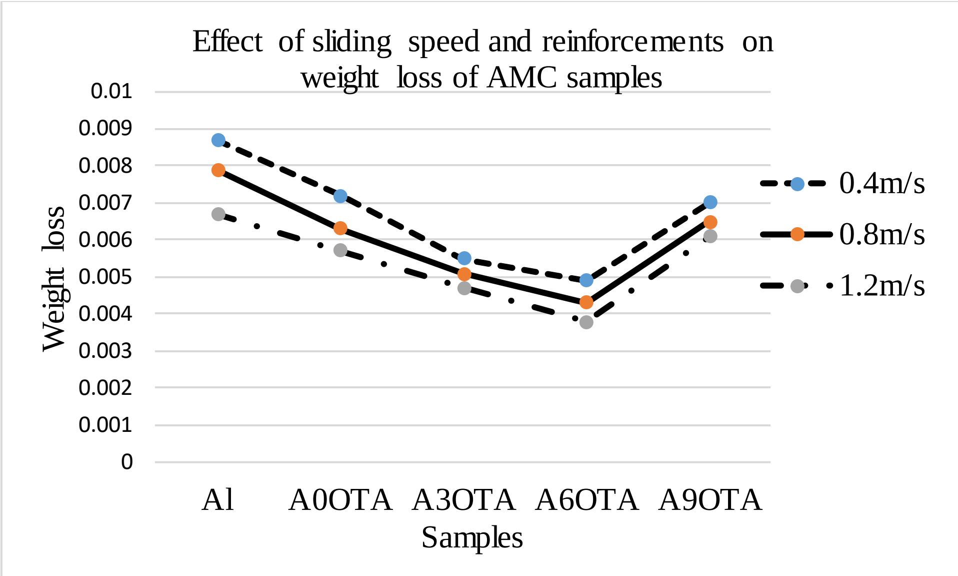

Figure 29. Effect of sliding speed and reinforcements on weight loss of AMC samples

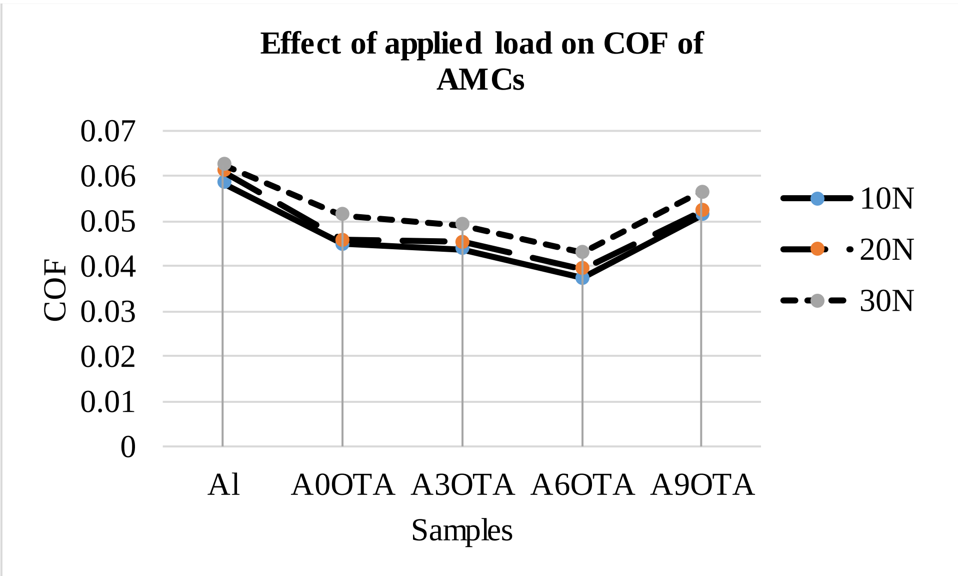

Figure 30. Coefficient of Friction Behavior of AMCs

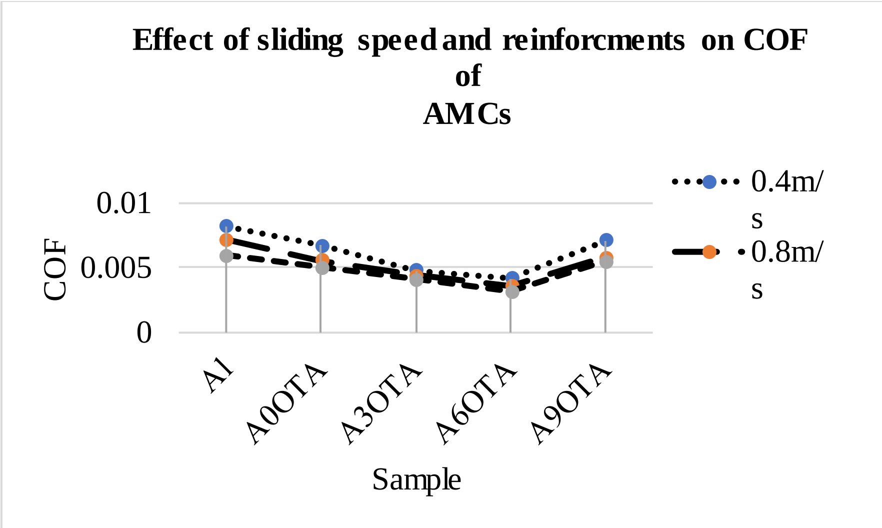

Figure 31. Effect of sliding speed and reinforcements on COF of AMCs

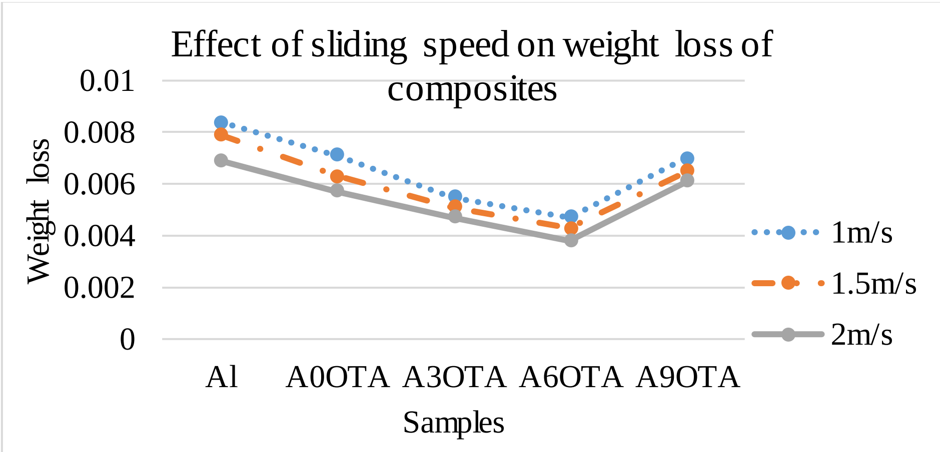

Figure 32. Effect of sliding speed on weight loss of composites

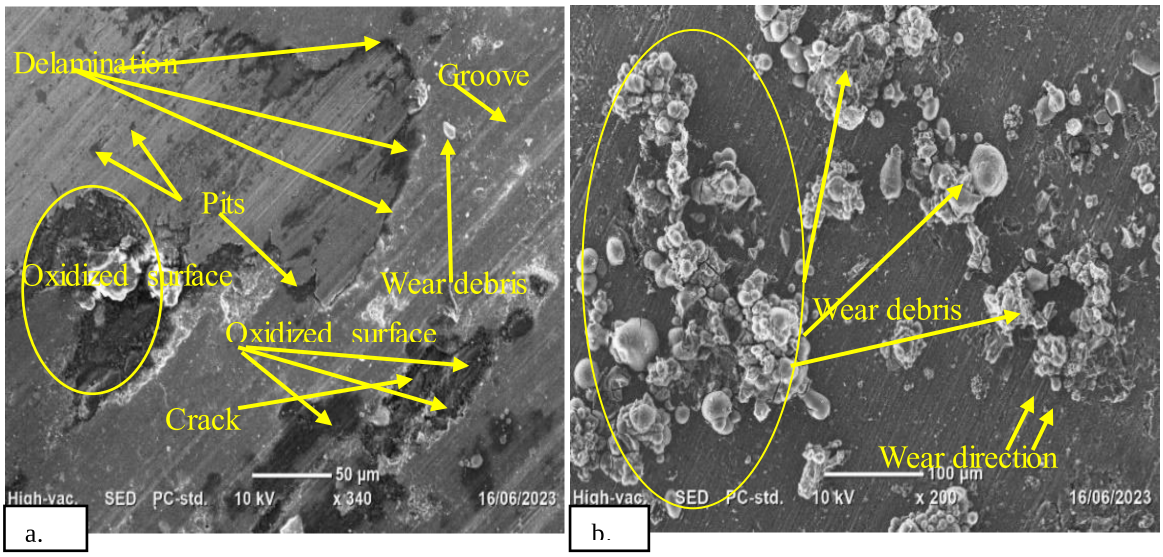

Figure 33. Morphology of wear samples, left Al and right 6wt.%OTA sintered at 500^{0}C

4.9 Corrosion Behaviour of AMCs

4.9.1 Potentiodynamic Polarization Technique

The potentiodynamic polarization test was used to examine the property of AMC samples in a 3.5% NaCl solution at ambient temperature. The curve below represents the Tafel polarization curves obtained from the Potentiodynamic polarization test. The corrosion potential (E_{corr}) and corrosion current density (I_{corr}), polarization resistance (R_P), and corrosion rate (C_R) extracted from the plots are reported in Table a) 19, b) 20 and c) 21. Also, the polarization resistance (RP) of samples was determined by the Stern–Geary equation

$$R_p = \frac{\beta_a \beta_c}{2.303I\,(\beta_a + \beta_c)} \ldots\ldots \quad (11)$$

Where, β_a and β_c are anodic and cathodic slopes of polarization curves, and improved corrosion resistance can be estimated by increasing the potential of corrosion, while the current density is reduced. High E_{corr} and low I_{cor}r indicate a low corrosion rate besides more uniform corrosion and high corrosion resistance function. The HAMC's inhibition efficiency (IE%) was calculated by the following equation:

$$Inhibitor\ Efficiency = \frac{I^0_{corr} - I_{corr}}{I^0_{corr}} \times 100 \ldots\ldots \quad (12)$$

Where, where $I^0{}_{corr}$ and I_{corr} represents the corrosion current density values of pure Al and AMCs, respectively.

As shown in figure 34 (a), (b) and (c) and Table 18, 19 and 20, the I_{corr} value of Al is the highest among the all samples in three batch, while the E_{corr} value is the lowest of all in three samples. This is due to the dissolution of the Al ions from the lattice into the solution and leads to thinning of the passive layer on the metal surface and ultimately increasing the corrosion rate in the base material. A potentiodynamic polarization test in an aerated 3.5% NaCl solution revealed that incorporating reinforcement particles into the base material (pure Al) caused the E_{corr} to move in the positive direction and the I_{corr} to decrease, as shown in Figure 26. Due to incorporation of OTA and additive the E_{corr} increased moderately almost in all samples, but decrease in I_{corr} higher than increase in $E_{corr.}$ and This is due new interface between aluminum and gr.

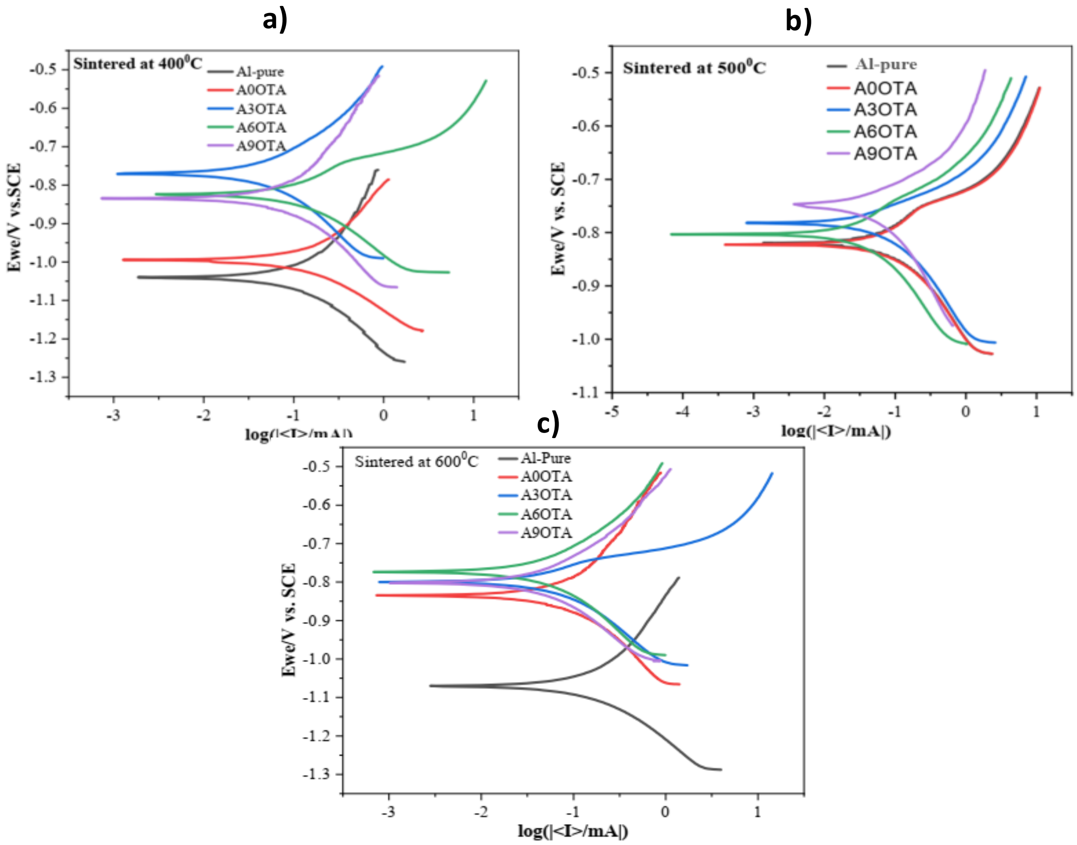

Figure 34. Graph of Potentiodynamic Polarization Technique for samples sintered at (a) 4000C (b) 500^0C and (c) 600^0C

Table 15. Corrosion extrapolation from figure 24 (a) of AMC Specimens sintered at 400^0C

Samples	**E_{corr}(mV)**	**I_{corr} (μA/cm^2)**	**$β_c$ (mV)**	**$β_a$ (mV)**	**R_P (Ω)**	**C_R (mmpy)**	**(IE%)**
Al-pure	-1006.407	128.095	126.8	228.0	27.62	1.77973	0.00
A0OTA	-1043.004	89.292	152.4	198.8	41.951	1.24061	30.29236
A3OTA	**-769.113**	**36.701**	**145.5**	**145.3**	**86.013**	**0.509918**	**71.3486**
A6OTA	-815.063	47.934	94.0	72.2	36.991	0.665987	62.57934
A9OTA	-831.860	59.586	159.4	186.3	62.5985	0.827879	53.482962

Table 16. Corrosion extrapolation from figure 2 (b) of AMC Specimens 500^0C

Samples	**E_{corr} (mV)**	**I_{corr} (μA/cm^2)**	**β_c (mV)**	**β_a (mV)**	**R_P (Ω)**	**C_R (mmpy)**	**(IE%)**
Al-pure	-807.206	79.915	169.2	82.0	29.2454	1.11033	0.00
A0OTA	-822.197	62.285	113.6	82.9	30.010	0.865378	22.06094
A3OTA	-780.464	43.757	110.0	69.2	42.15210	0.607953	45.24557
A6OTA	**-801.548**	**22.341**	**98.4**	**83.1**	**87.563**	**0.310402**	**72.0440**
A9OTA	-746.790	47.751	172.7	92.0	54.582	0.663445	40.24776

Table 17. Corrosion extrapolation from figure 24 (a) of AMC Specimens 600^0C

Samples	**E_{corr} (mV)**	**I_{corr} (μA/cm^2)**	**β_c (mV)**	**β_a (mV)**	**R_P (Ω)**	**C_R (mmpy)**	**IE (%)**
Al-pure	-1063.711	101.947	206.7	175.4	40.41333	1.41644	0.00
A0OTA	-837.751	117.954	258.3	380.1	56.614	1.63883	15.7013
A3OTA	-787.734	64.075	193.4	66.3	33.459	0.890248	37.14871
A6OTA	-763.971	57.090	220.2	188.7	77.2891	0.793199	44.00031
A9OTA	**-807.169**	**17.280**	**174.4**	**190.7**	**83.659**	**0.656901**	**83.05**

4.9.2 Electrochemical Impedance Spectroscopy Technique

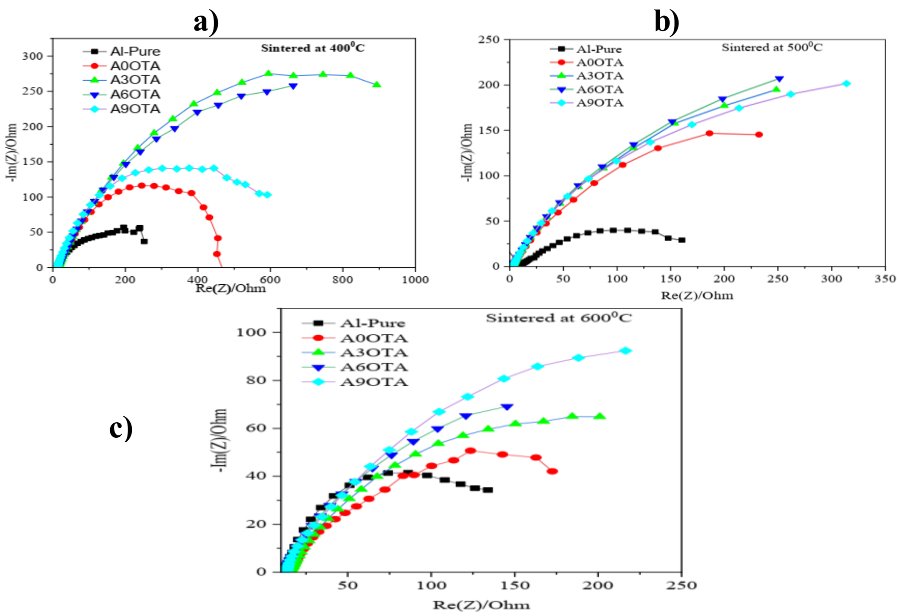

Figure 35. EIS Nyquist plots for pure Al and AMCs after 45minutes immersion in3.5%

a) A0OTA b) A3OTA

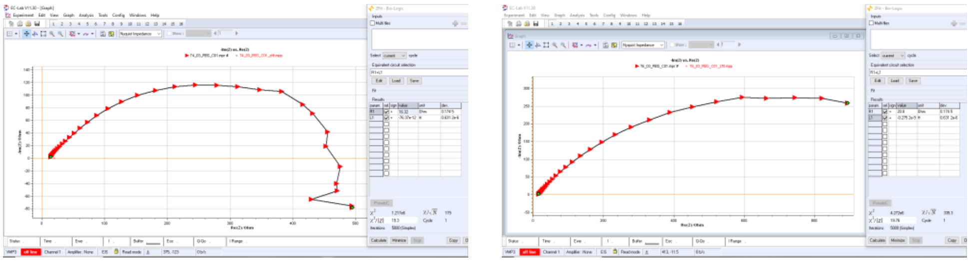

Figure 36 Z-fitting to the ENyquist plot for (400^0C) AMCs

a) A0OTA b) A6OTA

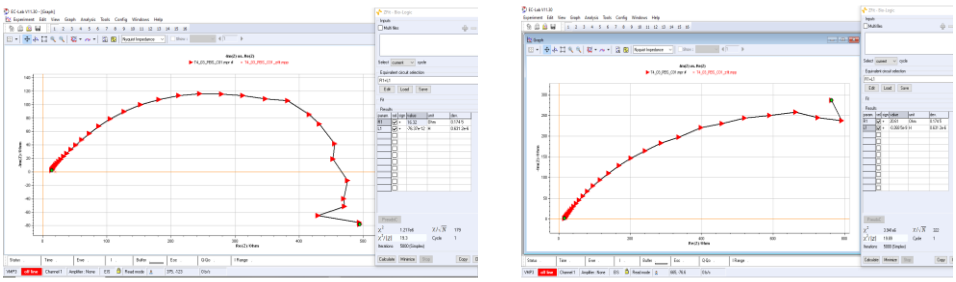

Figure 37. Z-fitting to the EIS Nyquist plot for (500^0C) AMCs

a) A0OTA b) A9OTA

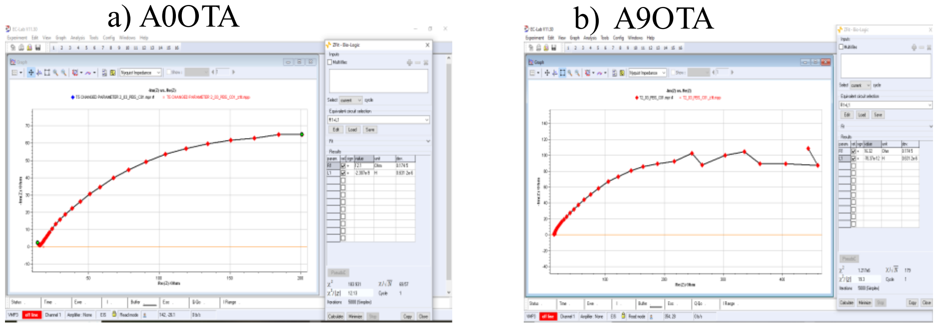

Figure 38. Z-fitting to the EIS Nyquist plot for (600^0C) AMCs

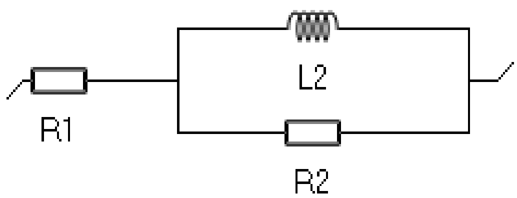

Figure 39. The equivalent circuit model used to fit the EIS experimental data for above figures 36, 37 and 38.

Table 18. EIS data combined with the equivalent circuit diagram in figure 36 and 39

Sample	**R_1 (Ω)**	**L_1(H)**	**R_2 (Ω**
Al-pure	15.24	$-9.995x10^{-9}$	3623
A0OTA	16.32	$-76.37x10^{-12}$	3731
A3OTA	**20.8**	**-0.275 2e-9**	**$1219x10^{2}$**
A6OTA	20.61	$-0.268\ 5x10^{-9}$	114350
A9OTA	18.48	$-0.785\ 1x10^{-9}$	$400x10^{2}$

Table 19. EIS data combined with the equivalent circuit diagram in figure 37 and 39

Sample	**R_1 (Ω)**	**L_2(H)**	**R_2 (Ω)**
Al-pure	1.23	$-65.15x10^{-6}$	7246
A0OTA	1.581	0.351121	7463
A3OTA	2.694	$-0.746\ 5x10^{-6}$	$2287x10^{2}$
A6OTA	**12.55**	**$-50.04x10^{-6}$**	**$2438x10^{2}$**
A9OTA	2.802	$-0.184\ 5x10^{-6}$	8012

Table 20. EIS data combined with the equivalent circuit diagram in figure 38 and39

Sample	**R_1 (Ω)**	**L_1(H)**	**R_2 (Ω**
Al-pure	7.39	3.22e15	7296
A0OTA	12.1	-2.307e-9	7482
A3OTA	13.71	-6.323e-9	8369
A6OTA	14.76	-18.75e-9	9786
A9OTA	**16.32**	**-76.37e-12**	**11861**

4.10 Taguchi based Grey Relational Analysis for Multi-Response Optimization of AMC process parameters

4.10.1 Measured Response Data

Below in the table 23 measured response datum of each L_{27} sample shown. Density and porosity are quality characteristic feature to be minimized, hence S/N must be smaller is better used. For hardness and compressive strength S/N larger is better used.

Table 21. Measured response data with Smaller is better quality.

	Experimental Density(g/cm³)			**Porosity (%)**		
Exp. No.	**ED-1**	**ED-2**	**ED-3**	**PO-1**	**PO-2**	**PO-3**
1	2.456	2.276	2.448	4.108	5.95	4.169
2	2.57	2.526	2.597	3.186	4.142	3.297
3	2.539	2.521	2.568	2.085	4.276	1.697
4	2.387	2.424	2.392	3.049	5.97	2.746
5	2.488	2.416	2.474	2.308	5.122	2.423
6	2.466	2.45	2.439	2.679	6.121	1.699
7	2.54	2.331	2.56	1.434	7.581	0.657
8	2.563	2.481	2.583	3.215	5.748	3.108
9	2.522	2.512	2.511	2.333	2.516	2.577
10	2.322	2.399	2.326	3.426	6.358	3.011
11	2.339	2.334	2.346	4.913	4.856	4.739
12	2.413	2.467	2.423	3.635	2.642	3.276
13	2.492	2.375	2.485	3.353	2.708	3.145
14	2.538	2.545	2.543	1.651	1.854	1.586
15	2.501	2.438	2.512	3.982	2.146	4.011
16	2.453	2.336	2.354	3.931	6.355	3.662
17	2.618	3.451	2.649	3.003	4.817	3.035
18	2.378	2.554	2.388	4.391	3.898	4.485
19	2.511	2.388	2.519	5.407	2.394	5.686
20	2.283	2.417	2.283	5.378	5.875	5.378
21	2.416	2.38	2.423	5.09	4.172	5.119
22	2.5	2.37	2.53	5.294	5.247	4.576
23	2.409	2.487	2.434	4.156	6.609	4.212
24	2.381	2.434	2.361	4.619	3.523	5.152
25	2.375	2.482	2.374	4.453	5.816	4.442
26	2.587	2.583	2.575	4.775	5.184	4.739
27	2.288	2.374	2.475	5.116	4.576	4.062

Table 22. Measured response data with Larger is better quality.

	Vickers Hardness			Compressive Strength		
Exp. No.	**HV-1**	**HV-2**	**HV-3**	**CS-1**	**CS-2**	**CS-3**
1	177.6	178.5	184.5	205.608	206.125	202.756
2	179.8	208.9	226.4	220.977	2210.58	223.789
3	208.9	222	239.2	226.497	222.136	225.475
4	335.7	332.5	337	236.643	235.235	224.369
5	300.6	297.7	308.7	226.696	236.237	229.159
6	259.2	277.5	257.6	230.924	231.147	227.969
7	356.6	355.3	325.7	291.9	293.741	290.916
8	329.1	387.7	326.8	286.976	288.321	287.274
9	405.6	386.3	344.2	292.447	289.447	291.654
10	198.5	224.5	212.3	283.544	285.635	281.523
11	242.7	247.8	245.6	270.364	271.126	272.864
12	248.5	247.1	217.1	256.786	257.632	25421.8
13	280.1	256.9	256.1	260.169	265.195	261.764
14	276.6	273.1	298.7	252.41	254.654	255.451
15	245.6	244.9	262.4	252.31	253.654	251.318
16	243.4	280.1	264	208.941	209.149	206.743
17	226.4	232.3	258.4	205.31	206.531	206.298
18	255.3	245.6	274.9	207.996	206.357	209.756
19	235	218.3	261.6	272.951	272.126	273.542
20	220.1	197.4	218.9	246.79	247.753	244.896
21	250.8	239.2	244.1	278.223	279.258	279.596
22	164.1	164.1	169	287.672	288.276	289.598
23	188.8	186.4	197.4	270.364	271.463	271.134
24	162.9	168.1	162.9	281.605	280.506	280.612
25	243.4	247.1	233	267.231	265.231	268.465
26	176.2	187.8	177.6	276.333	277.951	279.248
27	240.6	229.7	239.2	269.071	268.271	267.453

Taguchi based GRA for Multi-Response Optimization

In first step original response data must be converted to S/N ratio based on required quality characteristic feature. For each response, there were three replications. For Hardness and Compressive strength, the Larger is better used based on equation below.

$$S/N = -10 \log \frac{1}{3}\sum_{i=1}^{3}\frac{1}{Y_i^2} \quad \text{……(13)}$$

$$S/N = -10 \log \frac{1}{3}\sum_{i=1}^{3}Y^2 \quad \text{……(14)}$$

Table 23. S/N ratio (η) for each response value

S/N ratio (η) for each response value				
	Smaller is better		**Larger is better**	
Exp. No.	**ED**	**PO**	**HV**	**CS**
1	-7.48448	-13.65854	45.11139	46.19993
2	-8.12420	-11.04680	46.11676	46.67953
3	-8.06245	-9.29610	46.94053	47.15779
4	-7.62428	-12.42855	50.50221	47.24748
5	-7.79103	-10.96130	49.60666	47.28467
6	-7.81167	-11.99849	48.44258	47.21327
7	-7.73709	-13.00737	50.75510	49.21426
8	-8.03567	-12.47445	50.74871	49.06931
9	-8.01768	-7.88029	51.50366	49.18735
10	-7.46085	-13.09827	46.48413	49.11272
11	-7.37132	-13.69070	47.79537	48.54926
12	-7.74815	-10.13196	47.46433	48.10561
13	-7.72630	-9.77219	48.42191	48.41315
14	-8.10181	-4.61324	49.00936	48.09399
15	-7.85265	-10.85763	47.97918	47.98673
16	-7.58602	-13.63292	48.33930	46.31188
17	-9.69595	-11.40222	47.52703	46.16207
18	-7.84355	-12.59996	48.22427	46.43856
19	-7.78337	-13.50878	47.47111	48.79383
20	-7.42371	-14.88369	46.49916	47.77720
21	-7.59715	-13.64975	47.76778	48.70049
22	-7.73204	-14.06524	44.38570	49.08478
23	-7.77696	-14.18810	45.60677	48.71460
24	-7.63168	-13.03123	44.32751	48.85071
25	-7.70817	-13.88495	47.63823	48.60574
26	-8.24921	-13.81010	45.12073	48.87411
27	-7.35183	-13.26425	47.47106	48.53835
Min	**-9.69595**	**-14.88369**	**44.32751**	**46.16207**
Max	**-7.35183**	**-4.61324**	**51.50366**	**49.21426**

2. Normalize data: - Normalization is a transformation performed on a single input to distribute the data evenly and scale it into an acceptable range for further analysis. The S/N ratios obtained by Taguchi's method are normalized in the range of 0 and 1, and this procedure is known as grey relational.

Normalization Larger is the better manner, S/N ratio is performed using the below equation

$$z_{ij} = \frac{(\eta_{ij}) - \max(\eta_{ij})}{\max(\mu_{ij}) - \min(\mu_{ji})} \quad \ldots\ldots (15)$$

Normalization Smaller is the better manner, S/N ratio is performed using the below equation

$$z_{ij} = \frac{max\,(\eta_{ij}) - (\eta_{ij})}{\max(\eta_{ij}) - \min(\eta_{ji})} \quad \ldots\ldots (16)$$

Where, z_{ij}= Normalized value for i_{th} experiment for j_{th} dependent variable η_{ij} are the S/N ratio value to be normalized, and $max(\eta_{ij})$ and $\min(\eta_{ji})$ are the maximum and minimum values of η_{ji} respectively.

Table 24. Normalized S/N ratios (η) of the measured responses

Exp. No.	**Normalized S/N ratios (η) for smaller the better**		**Normalized S/N ratios (η) for larger is the better**	
	ED	PO	HV	CS
1	0.07143	0.88071	0.10923	0.01240
2	0.39128	0.62641	0.24933	0.16954
3	0.36040	0.45595	0.36413	0.32623
4	0.14133	0.76095	0.86045	0.35562
5	0.22470	0.61809	0.73565	0.36780
6	0.23502	0.71908	0.57344	0.34441
7	0.19773	0.81731	0.89569	1.00000
8	0.34701	0.76542	0.89480	0.95251
9	0.33802	0.31810	1.00000	0.99118
10	0.05962	0.82616	0.30053	0.96673
11	0.01485	0.88384	0.48325	0.78212
12	0.20326	0.53734	0.43712	0.63677
13	0.19234	0.50231	0.57056	0.73753
14	0.38008	0.00000	0.65242	0.63296
15	0.25551	0.60800	0.50886	0.59782
16	0.12220	0.87822	0.55905	0.04908
17	1.17711	0.66102	0.44586	0.00000
18	0.25096	0.77764	0.54302	0.09059
19	0.22087	0.86613	0.43806	0.86225
20	0.04105	1.00000	0.30262	0.52917
21	0.12776	0.87986	0.47940	0.83167
22	0.19521	0.92031	0.00811	0.95758
23	0.21767	0.93227	0.17827	0.83629
24	0.14503	0.81963	0.00000	0.88089
25	0.18327	0.90276	0.46135	0.80063
26	0.45378	0.89547	0.11054	0.88855
27	0.00511	0.84232	0.43806	0.77855
Min	**0.00000**	**0.00000**	**0.00000**	**0.00000**
Max	**1.00000**	**1.00000**	**1.00000**	**1.00000**

3. Calculation of the deviation sequences(Δ_{ij}) in both quality features is similar, and the equation is as follows; Δ = absolute difference between Z^0_{ij} and Z_{ij} which is a deviation from the target value and can be treated as a quality loss

$\boldsymbol{\Delta_{ij}} = ||\boldsymbol{Z^0_{ij}} - \boldsymbol{Z_{ij}}||$ Where Δ_{ij} is the deviation sequence, and Z^0_{ij} is usually equal to one ($Z^0_{ij} = 1$).

Table 25. Quality loss analysis with the respect to the normalized S/N ratios (η)

4. Calculation of the Grey relational coefficients (GRCs): Calculation of the grey relational co-efficient for the normalized S/N ratio values is based on the following equation

	Quality loss (Δ_{ij} has the same formula for all)			
Exp. No.	**ED**	**PO**	**HV**	**CS**
1	0.92857	0.11929	0.89077	0.98760
2	0.60872	0.37359	0.75067	0.83046
3	0.63960	0.54405	0.63587	0.67377
4	0.85867	0.23905	0.13955	0.64438
5	0.77530	0.38191	0.26435	0.63220
6	0.76498	0.28092	0.42656	0.65559
7	0.80227	0.18269	0.10431	0.00000
8	0.65299	0.23458	0.10520	0.04749
9	0.66198	0.68190	0.00000	0.00882
10	0.94038	0.17384	0.69947	0.03327
11	0.98515	0.11616	0.51675	0.21788
12	0.79674	0.46266	0.56288	0.36323
13	0.80766	0.49769	0.42944	0.26247
14	0.61992	1.00000	0.34758	0.36704
15	0.74449	0.39200	0.49114	0.40218
16	0.87780	0.12178	0.44095	0.95092
17	-0.17711	0.33898	0.55414	1.00000
18	0.74904	0.22236	0.45698	0.90941
19	0.77913	0.13387	0.56194	0.13775
20	0.95895	0.00000	0.69738	0.47083
21	0.87224	0.12014	0.52060	0.16833
22	0.80479	0.07969	0.99189	0.04242
23	0.78233	0.06773	0.82173	0.16371
24	0.85497	0.18037	1.00000	0.11911
25	0.81673	0.09724	0.53865	0.19937
26	0.54622	0.10453	0.88946	0.11145
27	0.99489	0.15768	0.56194	0.22145
Min	**0.00000**	**0.00000**	**0.00000**	**0.00000**
Max	**1.00000**	**1.00000**	**1.00000**	**1.00000**

$$GRC_{ij} = \frac{\Delta_{min} + \lambda\Delta_{m\grave{a}x}}{\Delta_{ij} + \lambda.\Delta_{max}}$$

$$Where, i = 1,2,3 \ldots \ldots \ldots .27\ experiments$$

$$j = 1,2,3 \ldots \ldots \ldots .27\ experiments \ldots\ldots\ldots\ldots\ldots\ldots\ldots\ldots\ldots \quad (17)$$

λ is the distinguishing coefficient, which is defined in the range $0 \leq \lambda \leq 1$ (the value may be changed depending on the system's actual needs). λ is also called the coefficient of identification, ranging between 0 and 1.

5. Compute the grey relational grade (GRG): After calculating the GRC_{ij}, the GRG_i can be obtained as follows

$$GRG_{ij} = \frac{1}{m}\Sigma GRC_{ji}$$

where m is the number of responses, and is equal to 4 namely; ED, PO, HV, and CS.

Table 26. Grey relational coefficients (GRCs) and grey relational grades (GRGs)

Grey Relational Coefficients (GRCs)					Grey Relational Grades (GRGs)	Rank
Exp. No.	**ED**	**PO**	**HV**	**CS**		
1	0.35000	0.80738	0.35951	0.33611	0.46576	26
2	0.45097	0.57235	0.39979	0.37581	0.50681	19
3	0.43875	0.47891	0.44019	0.42598	0.43888	27
4	0.36801	0.67654	0.78180	0.43692	0.55921	11
5	0.39206	0.56695	0.65415	0.44162	0.50637	20
6	0.39526	0.64027	0.53963	0.43268	0.49450	21
7	0.38394	0.73240	0.82739	1.00000	0.67701	1
8	0.43366	0.68066	0.82617	0.91326	0.66408	2
9	0.43030	0.42305	1.00000	0.98267	0.64610	3
10	0.34713	0.74202	0.41685	0.93761	0.54318	15
11	0.33667	0.81148	0.49176	0.69650	0.55811	13
12	0.38558	0.51939	0.47042	0.57922	0.59311	5
13	0.38236	0.50116	0.53796	0.65576	0.49282	22
14	0.44646	0.33333	0.58991	0.57668	0.46769	25
15	0.40177	0.56054	0.50447	0.55421	0.49196	23
16	0.36290	0.80414	0.53138	0.34461	0.50857	18
17	1.54851	0.59596	0.47432	0.33333	0.60168	4
18	0.40031	0.69218	0.52247	0.35476	0.48561	24
19	0.39089	0.78880	0.47084	0.78401	0.56585	9
20	0.34271	1.00000	0.41758	0.51502	0.55456	14

21	0.36437	0.80626	0.48991	0.74813	0.57605	7
22	0.38320	0.86253	0.33515	0.92179	0.57712	6
23	0.38991	0.88070	0.37829	0.75335	0.55872	12
24	0.36901	0.73490	0.33333	0.80761	0.52061	17
25	0.37973	0.83718	0.48139	0.71493	0.56364	10
26	0.47791	0.82709	0.35985	0.81774	0.57347	8
27	0.33447	0.76025	0.47083	0.69305	0.53993	16

6. Determine the optimal factor and its level combination. The higher grey relational grade implies a better product quality; therefore, based on the grey relational grade, the factor effect can be estimated and the optimal level for each controllable factor can also be determined.

1. Grouping of the grey relational grades by factor level for each column in the orthogonal array

2. Taking the average of grey relational grades

3. Calculation of grade values for each experiment of the L27 orthogonal array

To determine the effect of factor i, for example, we calculate the average of grade values (AGV) for each level j, represented as AGV_{ij}, and then the effect, E_i, is defined as:

$$E_i = \max(AGV_{ij}) - \min(AGV_{ij}) \quad (18)$$

Table 27. Response table of the average grey relational grade

Control factors	**Average Grey Relational by factor levels**			**Max-Min E(i)**	**Rank**
	1	**2**	**3**		
OTA	0.55097	0.52697	**0.55888**	0.03791	**3**
CP	0.53359	0.52053	**0.58446**	0.06393	**1**
ST	0.51820	**0.54795**	0.50668	0.04127	**2**
St	0.50455	**0.54041**	0.53276	0.03586	**4**

From table value, optimum composition OTA (9%), compacting pressure (60MPa), sintering temperature (500^{0}C) and sintering time(2hrs). From the rank we can understand that the most influencing was compacting pressure. Their sequence is as follows, CP >ST >OTA>St.

Table 28. Optimal parameter setting of HAMCs development

Optimum parameter values			
OTA - composition	**Compact pressure**	**Sintering Temperature**	**Sintering Time**
9%	60Mpa	500^0C	2hrs

Table 29. Confirmation test results

Sample	Avg. ED(g/cm^3)	Avg. PO. (%)	HV	CS(MPa)
Value	2.412	2.127	387.3	359.3

When the optimized value compared with other L_{27}`samples, the optimized has the highest values in all values. Hence, from the confirmation we can conclude that Taguchi based multi-response optimization is the best way to optimize output.

CHAPTER FIVE

5. CONCLUSIONS AND RECOMMENDATION

5.1 Conclusion

In this work, the investigation on the effect of Olive tree ash on Physio-Mechanical, Corrosion and Tribological properties of Aluminum matrix Composite via Powder metallurgy approach has been studied. The findings from this study are summarized below.

- ✓ Olive tree ash prepared successfully for reinforcement. The existence of important materials from OTA was confirmed but less in amount when compared with other solid agro-waste ash like bamboo ash, baggash ash, coconut ash and rise husk.
- ✓ Samples of OTA reinforced aluminum matrix composite prepared. Then characterization and testing has been done on prepared samples.
- ✓ When the physio-mechanical, wear, and corrosion behaviors of the Al(unreinforced) and fabricated aluminum matrix composites were compared, all reinforced composite samples showed better property than matrix material (Al).
- ✓ The phase analysis result indicated that Al peak dominated all other peaks because of its high intensity. When other peaks were minor. TGA/DTA result confirmed that thermal stability of produced composite was wide range and more stable than base material.
- ✓ Density of produced composite was decreased as OTA wt.% increases, and minimum porosity of composite obtained for A3OTA, A6OTA and A9OTA when sintered at 400^0C, 500^0C and 600^0C respectively. When OTA introduced hardness and compressive strength increased in all samples (samples sintered at 400^0C, 500^0C and 600^0C). From the three batch samples, the highest value of hardness and compressive strength found in third batch sample with 9wt.% OTA sintered at 600^0C (hardness=54.2% and compressive strength=52.5%) improved.
- ✓ The corrosion rate decreased and wear resistance increased as OTA composition increased up to some point then increased except third batch samples. In third batch as OTA increase, wear and corrosion both decreased in all samples. The corrosion inhibition efficiency (IE) increased up to 83% in third batch sample with 9wt.%OTA.
- ✓ Optimization result showed that compacting pressure is the most influencing factor (compacting pressure >> sintering temperature >> OTA composition >> sintering

time). According to optimized (confirmed) samples result, the physio-mechanical properties optimized sample was highest of other 27 samples, indicating that Taguchi based multi-response optimization was promising technique to improve output.

- ✓ When compared with base metal, new composite confirmed higher physio-mechanical, tribological and corrosion properties. Hence it will find potential application in automotive, aerospace, marine and others.
- ✓ Solid agro-waste materials are very important to reduce cost, composite weight and improve physio-mechanical, and tribological properties.

5.2 Recommendation

- ✓ To use aluminum alloy as matrix have better physical, mechanical, corrosion, and wear properties od composite.
- ✓ To increase required properties, use with additional ceramic reinforcement like Sic.
- ✓ To reduce porosity and to have good density using high compact pressure, above 60MPa.

REFERENCES

Akbar, H. I., Surojo, E., & Ariawan, D. (2020a). Investigation of industrial and agro wastes for aluminum matrix composite reinforcement. *Procedia Structural Integrity*, *27*, 30–37. https://doi.org/10.1016/j.prostr.2020.07.005

Akbar, H. I., Surojo, E., & Ariawan, D. (2020b). ScienceDirect ScienceDirect Investigation of Industrial and Agro Wastes for Aluminum Matrix Composite Reinforcement. *Procedia Structural Integrity*, *27*(2019), 30–37. https://doi.org/10.1016/j.prostr.2020.07.005

Akbar, H., Surojo, E., & Ariawan, D. (2020). Investigation of Industrial and Agro Wastes for Aluminum Matrix Composite Reinforcement. *Procedia Structural Integrity*, *27*, 30–37. https://doi.org/10.1016/j.prostr.2020.07.005

Alaneme, K. K., & Sanusi, K. O. (2015). Microstructural characteristics, mechanical and wear behaviour of aluminium matrix hybrid composites reinforced with alumina, rice husk ash and graphite. *Engineering Science and Technology, an International Journal*, *18*(3), 416–422. https://doi.org/10.1016/j.jestch.2015.02.003

Almomani, M. A., Hayajneh, M. T., & Al-Shrida, M. M. (2020). Investigation of mechanical and tribological properties of hybrid green eggshells and graphite-reinforced aluminum composites. *Journal of the Brazilian Society of Mechanical Sciences and Engineering*, *42*(1), 1–13. https://doi.org/10.1007/s40430-019-2130-z

Alshammari, B. A., Alotaibi, M. D., Alothman, O. Y., Lau, M. R. S., & Kian, K. (2019a). A New Study on Characterization and Properties of Natural Fibers Obtained from Olive Tree (Olea europaea L .) Residues. *Journal of Polymers and the Environment*, *27*(0123456789), 2334–2340. https://doi.org/10.1007/s10924-019-01526-8

Alshammari, B. A., Alotaibi, M. D., Alothman, O. Y., Lau, M. R. S., & Kian, K. (2019b). A New Study on Characterization and Properties of Natural Fibers Obtained from Olive Tree (Olea europaea L .) Residues. *Journal of Polymers and the Environment*, *27*(11), 2334–2340. https://doi.org/10.1007/s10924-019-01526-8

Ashebir, D. A., Mengesha, G. A., & Sinha, D. K. (2022a). An Insight into Mechanical and Metallurgical Behavior of Hybrid Reinforced Aluminum Metal Matrix Composite. *Advances in Materials Science and Engineering*, *2022*. https://doi.org/10.1155/2022/7843981

Ashebir, D. A., Mengesha, G. A., & Sinha, D. K. (2022b). The Role of Tetra Hybrid Reinforcements on the Behavior of Aluminum Metal Matrix Composites. *Journal of*

Nanomaterials, *2022*. https://doi.org/10.1155/2022/1988293

Ashebir, D. A., & Science, A. (2021). *Synthesis , Characterization and Testing of Self-Lubricating Tetra Hybrid Reinforced Al Matrix Composites via Powder Metallurgy Synthesis , Characterization and Testing of Self-Lubricating Tetra Hybrid Reinforced Al Matrix Composites via Powder Metallurgy*.

Aynalem, G. F. (2020). Processing Methods and Mechanical Properties of Aluminium Matrix Composites. In *Advances in Materials Science and Engineering* (Vol. 2020). Hindawi Limited. https://doi.org/10.1155/2020/3765791

Baradeswaran, A., & Perumal, A. E. (2014). Wear and mechanical characteristics of Al 7075/graphite composites. *Composites Part B: Engineering*, *56*, 472–476. https://doi.org/https://doi.org/10.1016/j.compositesb.2013.08.073

Bell, S., Davis, B., Javaid, A., & Essadiqi, E. (2006). *Final Report on Effect of Impurities in Aluminum*. https://doi.org/10.13140/RG.2.2.34366.28482

Buckner, C. A., Lafrenie, R. M., Dénommée, J. A., Caswell, J. M., Want, D. A., Gan, G. G., Leong, Y. C., Bee, P. C., Chin, E., Teh, A. K. H., Picco, S., Villegas, L., Tonelli, F., Merlo, M., Rigau, J., Diaz, D., Masuelli, M., Korrapati, S., Kurra, P., … Mathijssen, R. H. J. (2016). We are IntechOpen , the world ' s leading publisher of Open Access books Built by scientists , for scientists TOP 1 %. *Intech*, *11*(tourism), 13. https://www.intechopen.com/books/advanced-biometric-technologies/liveness-detection-in-biometrics

Cheah, L. (2010). *Cars on a Diet: The Material and Energy Impacts of Passenger Vehicle Weight Reduction in the US*.

Chen, C., Guo, Z., Luo, J., Wang, W., & Hao, J. (2016). No Title. *High Temperature Materials and Processes*, *35*(2), 169–175. https://doi.org/doi:10.1515/htmp-2014-0150

Composites, M. (2022). *Sensitivity Analysis of Reinforced Aluminum Based Metal*.

Czerwinski, F. (2021). *Current Trends in Automotive Lightweighting Strategies and Materials*.

Dev Srivyas, P., & Charoo, M. (2018). Role Of Fabrication Route On The Mechanical And Tribological Behavior Of Aluminum Metal Matrix Composites-A Review. In *Pranav Dev Srivyas et al./ Materials Today: Proceedings* (Vol. 5). www.sciencedirect.comwww.materialstoday.com/proceedings2214-7853

Dipl-ing, T. H., Dr-ing, T. W., & Dr-ing, T. S. (2012). *Graphite metal composites with*. *1*, 107–114.

Dwivedi, S. P., Srivastava, A. K., Maurya, N. K., & Sahu, R. (2020). Microstructure and mechanical behaviour of Al/SiC/agro-waste RhA hybrid metal matrix composite. *Revue Des Composites et Des Materiaux Avances*, *30*(1), 43–47. https://doi.org/10.18280/rcma.300107

Faleh, H., Muna, N., & Ştefănescu, F. (2015). Properties and Applications of Aluminium-Graphite Composites. *Advanced Materials Research*, *1128*, 134–143. https://doi.org/10.4028/www.scientific.net/amr.1128.134

Faleh, H., Muna, N., Ştefănescu, F., Noori, M., & Florin, Ștefănescu. (2015). Properties and Applications of Aluminium-Graphite Composites. *Advanced Materials Research*, *1128*, 134–143. https://doi.org/10.4028/www.scientific.net/amr.1128.134

Geng, L., & Huang, L. J. (2014). *Microstructures and Mechanical Hot Pressing*. *45*(December), 1965–1969. https://doi.org/10.1007/s11663-014-0203-z

Gürleme, A. (n.d.). *Effects of graphite on the corrosion behavior of aluminum – graphite composite in sodium chloride solutions*.

Hayajneh, M. T., Almomani, M. A., & Al-Shrida, M. M. (2019). Effects of waste eggshells addition on microstructures, mechanical and tribological properties of green metal matrix composite. *Science and Engineering of Composite Materials*, *26*(1), 423–434. https://doi.org/10.1515/secm-2019-0027

Ibhadode, A. O. A. (2022). Engine Lightweighting: Use of Green Materials as Reinforcement in Aluminum Metal Matrix Composites. In P. A. M. Nahhas & P. A. A. Ibhadode (Eds.), *Renewable Energy - Recent Advances*. IntechOpen. https://doi.org/10.5772/intechopen.108273

Jinfeng, L., Longtao, J., Gaohui, W., Shoufu, T., & Guoqin, C. (2009). Effect of Graphite Particle Reinforcement on Dry Sliding Wear of SiC/Gr/Al Composites. *Rare Metal Materials and Engineering*, *38*(11), 1894–1898. https://doi.org/https://doi.org/10.1016/S1875-5372(10)60059-8

John, M., & Menezes, P. L. (2021). Self-lubricating materials for extreme condition applications. *Materials*, *14*(19). https://doi.org/10.3390/ma14195588

Kanda, M., Puggal, S., Dhall, N., & Sharma, A. (2018). Recent Developments in the Fabrication, Characterization, and Properties Enhancement of Polymer Nanocomposites: A Critical Review. *Materials Today: Proceedings*, *5*(14, Part 2), 28243–28252. https://doi.org/https://doi.org/10.1016/j.matpr.2018.10.069

Karaoglu, S. Y., Karaoglu, S., & Unal, I. (2021). *International Journal of Aviation Aerospace Industry and Aluminum Metal Matrix Composites*. *2*(2), 73–81.

https://doi.org/10.23890/IJAST.vm02is02.0204

Kareem, A., Qudeiri, J. A., Abdudeen, A., Ahammed, T., & Ziout, A. (2021). A review on aa 6061 metal matrix composites produced by stir casting. *Materials*, *14*(1), 1–22. https://doi.org/10.3390/ma14010175

Khatkar, S. K., Suri, N. M., Kant, S., & Pankaj. (2018). A review on mechanical and tribological properties of graphite reinforced self lubricating hybrid metal matrix composites. *Reviews on Advanced Materials Science*, *56*(1), 1–20. https://doi.org/10.1515/rams-2018-0036

Kulkarni, P. P., Siddeswarappa, B., & Kumar, K. S. H. (2019). A Survey on Effect of Agro Waste Ash as Reinforcement on Aluminium Base Metal Matrix Composites. *Open Journal of Composite Materials*, *09*(03), 312–326. https://doi.org/10.4236/ojcm.2019.93019

Kumar, D., Pagar, D. D., Kumar, R., & Pruncu, C. I. (2019). Recent progress of reinforcement materials : a comprehensive overview of composite materials. *Integrative Medicine Research*, *x x*, 1–21. https://doi.org/10.1016/j.jmrt.2019.09.068

Kumar, N., & Bharti, A. (2021). Powder Compaction Dies and Compressibility of Various Materials. *Powder Metallurgy and Metal Ceramics*, *60*, 403–409. https://doi.org/10.1007/s11106-021-00253-x

Kumar, N., & Bharti, A. (2022). Optimization of powder metallurgy process parameters to enhance the mechanical properties of AZ91 magnesium alloy. *Materials Physics and Mechanics*, *48*(3), 315–327. https://doi.org/10.18149/MPM.4832022_3

Kumar Sharma, A., Bhandari, R., Aherwar, A., Rimašauskienė, R., & Pinca-Bretotean, C. (2020). A study of advancement in application opportunities of aluminum metal matrix composites. *Materials Today: Proceedings*, *26*, 2419–2424. https://doi.org/https://doi.org/10.1016/j.matpr.2020.02.516

Lakshmi Narayana, K. S., Benal, M. M., & Shivanand, H. K. (2021). Effect of graphite on aluminium matrix composites fabricated by stir casting route – A review. *Materials Today: Proceedings*, *45*, 327–331. https://doi.org/https://doi.org/10.1016/j.matpr.2020.11.051

Lindroos, V. K., & Talvitie, M. J. (1995). Recent advances in metal matrix composites. *Journal of Materials Processing Technology*, *53*(1), 273–284. https://doi.org/https://doi.org/10.1016/0924-0136(95)01985-N

Liu, Z., Zu, G., Luo, H., Liu, Y., & Yao, G. (2010). Influence of Mg addition on graphite particle distribution in the Al alloy matrix composites. *Journal of Materials Science* *and Technology*, *26*(3), 244–250. https://doi.org/10.1016/S1005-0302(10)60041-2

Loganathan, S., Valapa, R. B., Mishra, R. K., Pugazhenthi, G., & Thomas, S. (2017). Thermogravimetric Analysis for Characterization of Nanomaterials. In *Thermal and Rheological Measurement Techniques for Nanomaterials Characterization* (Vol. 3). Elsevier Inc. https://doi.org/10.1016/B978-0-323-46139-9.00004-9

Miller, W. S., Zhuang, L., Bottema, J., Wittebrood, A. J., & Smet, P. De. (2000). *Recent development in aluminium alloys for the automotive industry*. *280*, 37–49.

Mohanavel, V., Rajan, K., Kumar, S. S., Vijayan, G., Vijayanand, M. S., Suresh Kumar, S., Vijayan, G., & Vijayanand, M. S. (2018). Study on mechanical properties of graphite particulates reinforced aluminium matrix composite fabricated by stir casting technique. *Materials Today: Proceedings*, *5*(1), 2945–2950. https://doi.org/10.1016/j.matpr.2018.01.090

Mussatto, A., Ahad, I. U. I., Mousavian, R. T., Delaure, Y., & Brabazon, D. (2021). Advanced production routes for metal matrix composites. *Engineering Reports*, *3*(5), 1–25. https://doi.org/10.1002/eng2.12330

Nturanabo, F., Leonard Masu and John Baptist Kirabira, Masu, L., Baptist Kirabira, J., & Kirabira, J. B. (2020). Novel Applications of Aluminium Metal Matrix Composites. *Aluminium Alloys and Composites*, *i*, 13. https://doi.org/10.5772/intechopen.86225

Nturanabo, F., Masu, L., & Baptist Kirabira, J. (2020). Novel Applications of Aluminium Metal Matrix Composites. *Aluminium Alloys and Composites*. https://doi.org/10.5772/intechopen.86225

Nturanabo, F., Masu, L., & Kirabira, J. (2019). *Novel Applications of Aluminium Metal Matrix Composites*. https://doi.org/10.5772/intechopen.86225

Omran, S. H., Al-masoudy, M. M., Hassoon, O. H., & Mohammed, A. (2022). *Optimization of mechanical wear resistance for recycled (Al-Mg-Si) reinforced SiC composite material using PM method*. 295–303.

Omrani, E., Moghadam, A. D., Menezes, P. L., & Rohatgi, P. K. (2016). Influences of graphite reinforcement on the tribological properties of self-lubricating aluminum matrix composites for green tribology, sustainability, and energy efficiency—A review. *International Journal of Advanced Manufacturing Technology*, *83*(1–4), 325–346. https://doi.org/10.1007/s00170-015-7528-x

Orhadahwe, T. A., Ajide, O. O., Adeleke, A. A., & Ikubanni, P. P. (2020). A review on primary synthesis and secondary treatment of aluminium matrix composites. *Arab Journal of Basic and Applied Sciences*, *27*(1), 389–405.

https://doi.org/10.1080/25765299.2020.1830529

Ozturk, M., Altay, V., Gönenç, T. M., Unal, B. T., Efe, R., Akçiçek, E., & Bukhari, A. (2021). An overview of olive cultivation in Turkey: Botanical features, eco-physiology and phytochemical aspects. *Agronomy*, *11*(2), 1–26. https://doi.org/10.3390/agronomy11020295

Panda, B., Niranjan, C. A., Vishwanatha, A. D., Harisha, P., Chandan, K. R., & Kumar, R. (2019). Development of Novel Stir Cast Aluminium Composite with modified Coconut Shell Ash Filler. *Materials Today: Proceedings*, *22*, 2715–2724. https://doi.org/10.1016/j.matpr.2020.03.402

Parveez, B., Maleque, M. A., & Jamal, N. A. (2021). Influence of agro-based reinforcements on the properties of aluminum matrix composites: a systematic review. In *Journal of Materials Science* (Vol. 56, Issue 29, pp. 16195–16222). Springer. https://doi.org/10.1007/s10853-021-06305-2

Rahman, M. A., Haque, S., Manokar, M., Mohamed, A., & Kamaludeen, B. (2023). A review of environmental friendly green composites : production methods , current progresses , and challenges. *Environmental Science and Pollution Research*, 16905–16929. https://doi.org/10.1007/s11356-022-24879-5

Rajak, D. K., Pagar, D. D., Kumar, R., Pruncu, C. I., Kumar, D., Pagar, D. D., Kumar, R., & Pruncu, C. I. (2019). Recent progress of reinforcement materials: A comprehensive overview of composite materials. *Journal of Materials Research and Technology*, *8*(6), 6354–6374. https://doi.org/10.1016/j.jmrt.2019.09.068

Raju, P. (2019). Fabrication and Analysis of Aluminium based Metal Matrix Composites Reinforced with Aluminium Oxide. In *International Journal of Engineering Research & Technology* (Vol. 7, Issue 06). www.ijert.org

Ramanathan, A., Krishnan, P. K., & Muraliraja, R. (2019). A review on the production of metal matrix composites through stir casting – Furnace design, properties, challenges, and research opportunities. *Journal of Manufacturing Processes*, *42*(June), 213–245. https://doi.org/10.1016/j.jmapro.2019.04.017

Ravichandran, M., Anandakrishnan, V., & Introduction, I. (2015). *Optimization of powder metallurgy parameters to attain maximum strength coef fi cient in Al – 10 wt % MoO 3 composite*. https://doi.org/10.1557/jmr.2015.211

Ravindran, P., Jinnah Sheik Mohamed, M., Joe Patrick Gnanaraj, S., & Appadurai, M. (2022). Effect of graphite addition on dry sliding wear behavior of Self-lubricating Al-SiC-Gr hybrid composites by PM process. *Materials Today: Proceedings*, *60*, 783–

787. https://doi.org/https://doi.org/10.1016/j.matpr.2021.09.198

Rohatgi, P. K. (n.d.). *Self-Lubricating Composites*.

Saini, S., Gupta, A., Jyoti, A., & Sumit, M. (2022). Rice husk - extracted silica reinforced graphite / aluminium matrix hybrid composite. *Journal of Thermal Analysis and Calorimetry*, *147*(2), 1157–1166. https://doi.org/10.1007/s10973-020-10404-8

Samal, P., Vundavilli, P. R., Meher, A., & Mahapatra, M. M. (2020). Recent progress in aluminum metal matrix composites: A review on processing, mechanical and wear properties. *Journal of Manufacturing Processes*, *59*, 131–152. https://doi.org/https://doi.org/10.1016/j.jmapro.2020.09.010

Sangghaleh, A., & Halali, M. (2009). Effect of magnesium addition on the wetting of alumina by aluminium. *Applied Surface Science*, *255*(19), 8202–8206. https://doi.org/10.1016/j.apsusc.2009.05.044

Sankhla, A. M., Patel, K. M., Makhesana, M. A., Giasin, K., Pimenov, D. Y., Wojciechowski, S., & Khanna, N. (2022). Effect of mixing method and particle size on hardness and compressive strength of aluminium based metal matrix composite prepared through powder metallurgy route. *Journal of Materials Research and Technology*, *18*, 282–292. https://doi.org/https://doi.org/10.1016/j.jmrt.2022.02.094

Seetharaman, S., & Gupta, M. (2021a). Fundamentals of Metal Matrix Composites. In *Reference Module in Materials Science and Materials Engineering*. https://doi.org/10.1016/B978-0-12-803581-8.00001-1

Seetharaman, S., & Gupta, M. (2021b). *Provided for non-commercial research and educational use . January*. https://doi.org/10.1016/B978-0-12-803581-8.00001-1

Seetharaman, S., Subramanian, J., Singh, R. A., Wong, W. L. E., Nai, M. L. S., & Gupta, M. (2022). Mechanical Properties of Sustainable Metal Matrix Composites: A Review on the Role of Green Reinforcements and Processing Methods. *Technologies*, *10*(1), 32. https://doi.org/10.3390/technologies10010032

Seshappa, A., & Anjaneya Prasad, B. (2021). Characterization and Investigation of Mechanical Properties of Aluminium Hybrid Nano-composites: Novel Approach of Utilizing Silicon Carbide and Waste Particles to Reduce Cost of Material. *Silicon*, *13*(12), 4355–4369. https://doi.org/10.1007/s12633-020-00748-z

Shahid, R. N., & Scudino, S. (2018). Microstructure and mechanical behavior of al-mg composites synthesized by reactive sintering. *Metals*, *8*(10). https://doi.org/10.3390/met8100762

Shanmugavel, R., Chinthakndi, N., Selvam, M., & Madasamy, N. (2022). *Al-Mg-MoS 2*

Reinforced Metal Matrix Composites :

Sharma, A. K., Bhandari, R., Aherwar, A., Rimašauskiene, R., & Pinca-Bretotean, C. (2020a). A study of advancement in application opportunities of aluminum metal matrix composites. *Materials Today: Proceedings*, *26*(xxxx), 2419–2424. https://doi.org/10.1016/j.matpr.2020.02.516

Sharma, A. K., Bhandari, R., Aherwar, A., Rimašauskiene, R., & Pinca-Bretotean, C. (2020b). A study of advancement in application opportunities of aluminum metal matrix composites. *Materials Today: Proceedings*, *26*, 2419–2424. https://doi.org/10.1016/j.matpr.2020.02.516

Sharma, P., Sharma, S., & Khanduja, D. (2016). Effect of graphite reinforcement on physical and mechanical properties of aluminum metal matrix composites. *Particulate Science and Technology*, *34*(1), 17–22. https://doi.org/10.1080/02726351.2015.1031924

Sharma, P., Sharma, S., Kumar Garg, R., Paliwal, K., Khanduja, D., & Dabra, V. (2017). Effect of Graphite Content on Mechanical Properties and Friction Coefficient of Reinforced Aluminum Composites. *Powder Metallurgy and Metal Ceramics*, *56*(5–6), 264–272. https://doi.org/10.1007/s11106-017-9894-4

Sharma, S., Saxena, K., & Kumar, N. (2022). Effect of SiC on Mechanical Properties of Al-Based Metal Matrix Composites Produced by Stir Casting. *Metal Science and Heat Treatment*, *64*, 316–320. https://doi.org/10.1007/s11041-022-00807-9

Shinde, D. M., Sahoo, P., & Davim, J. P. (2020). Tribological characterization of particulate-reinforced aluminum metal matrix nanocomposites: A review. *Advanced Composites Letters*, *29*, 1–28. https://doi.org/10.1177/2633366X20921403

Singh, G., Giri, T., & Noori, Q. (2017). REVIEW PAPER ON FABRICATION OF ALUMINUM MAGNESIUM COMPOSITE MATERIAL. In *European Journal of Material Sciences* (Vol. 4, Issue 2). www.eajournals.org

Singh, J., & Chauhan, A. (2015). Characterization of hybrid aluminum matrix composites for advanced applications – A review. *Integrative Medicine Research*, *5*(2), 159–169. https://doi.org/10.1016/j.jmrt.2015.05.004

Singh, L., Ram, B., Singh, A., & Sahib, F. (2013). *OPTIMIZATION OF PROCESS PARAMETER FOR STIR CASTED ALUMINIUM METAL MATRIX COMPOSITE USING TAGUCHI METHOD*. 375–383.

Srinivasan, R., Vignesh, S. B., Veeramanipandi, P., Sabarish, M., & Yuvaraj, C. S. (2020). Materials Today: Proceedings Experimental investigation on aluminium hybrid metal matrix composites fabricated through stir casting technique. *Materials Today: Proceedings*, *xxxx*. https://doi.org/10.1016/j.matpr.2020.03.810

Srivastava, A. (2017). Recent Advances in Metal Matrix Composites (MMCs): A Review. *Biomedical Journal of Scientific & Technical Research*, *1*(2), 1–4. https://doi.org/10.26717/bjstr.2017.01.000236

Srivyas, P. D., & Charoo, M. S. (2018). Role of Reinforcements on the Mechanical and Tribological Behavior of Aluminum Metal Matrix Composites - A Review. *Materials Today: Proceedings*, *5*(9), 20041–20053. https://doi.org/10.1016/j.matpr.2018.06.371

Stalin, B., Sudha, G. T., & Ravichandran, M. (2020). ScienceDirect Optimization of Powder Metallurgy Parameters for AA7072-MoO 3 Composites through Taguchi Method. *Materials Today: Proceedings*, *22*, 2622–2630. https://doi.org/10.1016/j.matpr.2020.03.393

Sudha, G. T., Stalin, B., & Ravichandran, M. (2019). *Optimization of powder metallurgy parameters to obtain low corrosion rate and high compressive strength in Al-MoO 3 composites using SN ratio and ANOVA analysis Optimization of powder metallurgy parameters to obtain low corrosion rate and high compressive*.

Surappa M.K. (2003). Aluminium Matrix Composites: Challenges and Opportunities // Sadhana. Department of Metallurgy, Indian Institute of Science, Bangalore 560 012, India. *S¯Adhan¯A*, *28*(1–2), 319–334.

Taiwo, O. O., Osoba, L. O., Adewunmi, O. O., & Adeosun, S. O. (2020). *A Study on Mechanical Properties of Aluminum-Graphite and Aluminum-Graphite- Zircon Hybrid Composites*. *48*(2), 12–20.

Téllez-Villaseñor, M. A., León-Patiño, C. A., Aguilar-Reyes, E. A., & Bedolla-Jacuinde, A. (2021). Effect of load and sliding velocity on the wear behaviour of infiltrated TiC/Cu–Ni composites. *Wear*, *484–485*, 203667. https://doi.org/https://doi.org/10.1016/j.wear.2021.203667

Torralba, J. M., Costa, C. E., & Velasco, F. (2003). *P / M aluminum matrix composites : an overview*. *133*, 203–206.

Vani, V. V., & Chak, S. K. (2018). The effect of process parameters in Aluminum Metal Matrix Composites with Powder Metallurgy. In *Manufacturing Review* (Vol. 5). EDP Sciences. https://doi.org/10.1051/mfreview/2018001

Velusamy, S., Subbaiyan, A., Murugesan, S. R., Shanmugamoorthy, M., Sivakumar, V., Velusamy, P., Veerasamy, S., Mani, K., Sundararaj, P., & Periyasamy, S. (2022). *Comparative Analysis of Agro Waste Material Solid Biomass Briquette for*

Environmental Sustainability. *2022*.

Vijayakumar, S., Kumar, P. S. S., Sampath, P., Manickam, S., Ramaiah, G. B., & Pydi, H. P. (2022). *The Effect of Stir-Squeeze Casting Process Parameters on Mechanical Property and Density of Aluminum Matrix Composite*. *2022*.

Vijayaram, D. T. R., & Baskaralal, V. P. M. (2016). A Review on the Processing Methods, Properties and Applications of Metal Matrix Composites. *International Journal of Engineering Research and Technology*, *9*(1), 45–51. www.rsisinternational.org

Virkunwar, A. K., Ghosh, S., & Basak, R. (2018). *Study of Mechanical and Tribological Characteristics of Aluminium Alloy Reinforced with Sugarcane Bagasse Ash*. https://ssrn.com/abstract=3313510

Wang, L., Sun, Y., Bo, L., Zuo, M., & Zhao, D. (2019). Effects of melt cooling rate on the microstructure and mechanical properties of Al-Cu alloy. *Materials Research Express*, *6*. https://doi.org/10.1088/2053-1591/ab44eb

Yamagata, H. (2003). Metal matrix composites in motorbikes. In *Metal and Ceramic Matrix Composites*. https://doi.org/10.1887/0750308729/b1149c3

Yekinni, A. A., Bello, S. K., Bajela, G. G., & Adigun, I. A. (2020). Effect of Coconut Shell Ash and Graphite Particles on Microstructure and Mechanical Properties of Recycled Aluminium Composites. *International Journal of Advances in Scientific Research and Engineering*, *06*(10), 61–71. https://doi.org/10.31695/ijasre.2020.33904

You, A., Be, M. A. Y., In, I., Fayomi, O. S. I., Sojobi, J. W., Nkiko, M. O., Akande, I. G., & Noiki, A. A. (2022). An overview of the influence of agro waste reinforcement on aluminium matrix composites. *TECHNOLOGIES AND MATERIALS FOR RENEWABLE ENERGY, ENVIRONMENT AND SUSTAINABILITY: TMREES21Gr*, *2437*(August), 020123. https://doi.org/10.1063/5.0093172

Zeren, A. (2015). Effect of the graphite content on the tribological properties of hybrid Al/SiC/Gr composites processed by powder metallurgy. *Industrial Lubrication and Tribology*, *67*(3), 262–268. https://doi.org/10.1108/ILT-07-2014-0066

Zhang, A., & Li, Y. (2023). *Thermal Conductivity of Aluminum Alloys — A Review*.

Zhang, W., & Xu, J. (2022). Advanced lightweight materials for Automobiles: A review. *Materials & Design*, *221*, 110994. https://doi.org/https://doi.org/10.1016/j.matdes.2022.110994

Research Fund Acknowledgement

This research thesis was funded by Adama Science and Technology University under the grant number of ASTU/SM-R/749/23, Adama, Ethiopia.